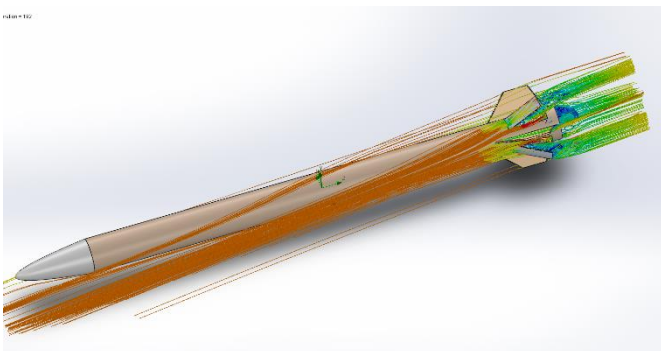




Design 1 Airbrakes Team Submission 2



Contents

Section 1- Executive Summary:	3
1.1: Context	3
1.2: Subject, describe the project and why. The problem we want to solve	3
1.3: Purpose of report	3
1.4: Methods of analysis, what we did and how we did it	3
1.5: Results	4
1.6: Conclusions	4
1.7: Recommendations	4
1.8: Limitations	4
Section 2- Summary of previous submission	5
Section 3- Final Design:	8
3.1: Test Rocket Criteria	8
3.2: Final Design	8
3.2.1- Design Overview	8
3.2.2: Changes from first submission	11
3.2.3: Mechanical actuation system:	12
3.3- Rocket Avionics Systems:	16
3.3.1- Hardware	16
3.3.2- Software	18
Section 4- Design Performance:	20
4.1- Simulated Performance:	20
Section 5- Manufacturing Methods	30
5.1: Fin manufacturing - Thomas Mackellar	30
5.2: Avionics Sed- Siddhant Tandon	31
5.3: 3D Printed ABS Cams - Nicole Tryndoch	32
Section 6-References	30
Appendices	34
Appendix A: Budget and Cost Breakdown	34
Appendix B: Material Choices for various components	35

Section 1- Executive Summary:

1.1: Context

The aerospace industry has been utilising air brakes to control vehicle trajectory for decades. With space travel gaining increased recognition in recent years, advancing aerospace technology is crucial to reach these milestones. While rockets have yet to carry passengers on flights into space, the industry hopes to make this a possibility in the near future. In order to control yaw and pitch, these future vehicles will require an external system that can be deployed and retracted as required.

Aeroplanes are able to alter altitude, increasing lift or downward force to take off and land respectively. This is possible through the use of mechanical flaps on the wings, which are deployed at low altitudes and moved up or down as required.

A similar design may be utilised in rockets.

1.2: Subject, describe the project and why. The problem we want to solve

Flying to a prescribed altitude is a major requirement at Australian Rocketry Competitions. Monash High Powered Rocketry (HPR) has posed the challenge to implement an autonomous altitude altering system into their future designs, one that will react to changes in atmospheric and meteorological conditions, and be able to alter the trajectory to reach the desired altitude.

One such method is using an air braking system, which can be deployed when required to decrease the rocket's acceleration. A successful design will be altered and utilised in HPR's future rockets.

The purpose of this project is to design, build, and test air brakes on a level one rocket. Full autonomy will be implemented at a later date, thus the only requirement of the brakes is that they significantly slow down the rocket. To test this, the brakes were to be programmed to deploy after burnout, remain opened for a minimum of two seconds, and fully retract for the remaining duration of the flight.

1.3: Purpose of report

This report outlines the process in which a functional air braking system was designed, built, and tested. All decisions are explained, as well as analysed for positive and negative aspects. The primary goal of the report is to show how to implement this design in a rocket, so it can be recreated in future builds.

1.4: Methods of analysis, what we did and how we did it

Prior to launch, several simulations were conducted to predict the results of both the rocket with air brakes, and without. An Open Rocket simulation provided values for flight without air brakes, and these values were used as the basis of comparison of air brake performance. A CFD analysis of the air brakes showed how air flow would affect the rocket's stability and flight.

On launch day, flight data was measured using a suite of onboard avionics sensors, and saved to an SD card. An accelerometer recorded acceleration over time, and an altimeter recorded height and velocity. All the data combined gave a wide overview of the flight.

1.5: Results

Comparing a simulation from Open Rocket, to data collected from the accelerometer and altimeter during the flight, the apogee was approximately 900 ft lower than predicted. The maximum height of the rocket was predicted to reach 2640 ft, whereas with air brake deployment, only reached 1722 ft.

The drag on the panels was found to be 30.1N, having increased 2.3 times from 13.5N without air brakes.

1.6: Conclusions

The projective objective was to implement an air braking system that would significantly decelerate the rocket. Given that the apogee was found to be approximately 900 ft lower than predicted, the project was a success. With a simple design that can easily be modified to fit into future rockets, and the ability to implement a fully autonomous system that will react to changing conditions, HPR will benefit from the research and data collected in this report.

1.7: Recommendations

For future implementations of this s\design, a few modifications and alterations ought to be made to insure maximum efficiency.

To maximise drag and increase deceleration, the brake panels should be opened to the largest angle possible. This can be achieved through using a 180 degree servo rather than the 120 degree servo that was used for this project.

The system can be modified to deploy the brake panels independently if, rather than using one large servo, it uses three smaller ones. This was not a viable option in this project due to limited space within the phenolic body tube. In larger rockets, there will be sufficient space to fit the modified system.

In the current model, the electronics in the nose cone are connected to the actuation system through a 5m long wire. This may pose issues with signal loss or tangling of the parachute.

Therefore, a braking wire may be used in future adaptations of this design.

Upon landing, one of the brake panels detached. This was found to be an issue with adhesion. Future designs ought to significantly score the panels before using a high strength epoxy resin to attach them. Furthermore, an alternative to the small magnets may be used to keep the panels closed during descent. Stronger magnets, springs, or electromagnets are suitable options.

1.8: Limitations

The brakes have been designed to be positioned between the fins, with the servo mounted just above the motor deployment charge. As the servo mount obstructs access between the charge and the parachute, an alternative will need to be utilised to deploy the parachute.

This design can be altered to control pitch and yaw, however, roll cannot be controlled.

Section 2- Summary of previous submission

The previous report explored possible design choices for a fully functioning air braking system, with retractable air brakes that would deploy after burnout to significantly reduce the acceleration of the rocket. Design choices were scrutinised for best possible performance, as well as safety and efficiency. Other factors included practically, capability of the team, and timeliness.

The first section covered background research on fundamental rocket dynamics, methods of mechanical actuation, and electrical and sensor systems. Basic dynamics were researched in order to understand how air brakes would affect the rocket's stability and trajectory. It was important to understand how much drag would be acting on the rocket, and thus the air brakes. Fluid properties explained the boundary layer, and if the brakes would interfere with the fins. The electrical background research covered both required electronics on board, and electronics relating to the air braking mechanism.

An OFFERS analysis was conducted to decide on the basic criteria and limitations of the project. The objective was "To design and implement a mechanically actuated system that slows down a rocket."

Functions documented the entire process of the air brakes from launch to landing. This covered the required actions for the system. Factors introduced limitations and requirements to be followed throughout the project. This included {wo}man power, money, machines, methods, minutes, and materials. Effects listed what would come out from completing the project, what HPR will gain from a successful air braking mechanism.

Requirements and specifications were organised in a table, stating the performance, appearance, safety, and cost requirements. Criteria specifies what requirement entitles, and specifications attach a value. Finally, weight states how important that requirement is in conjunction to the others, giving it a score out of 10, with 1 being of little importance, and 10 being a necessity. The OFFERS section narrowed down the project into components, a simple way to see what had to be designed, and what had to be taken into consideration.

Required functions of the mechanism were outlined in a table, with potential solutions listed for each. This was the concept generation table. Combinations of alternatives were considered, presenting a number of options for the final design. This also allowed for the team to consider what they wanted the mechanism to accomplish, and which alternatives were the most suitable.

From the concept generation table, three designs were proposed; holes in the nose cone, radially deployed flaps, and flaps between fins. Each design was scrutinised in terms of design, advantages, and disadvantages.

The first design, as seen in figure 2.1, proposed four equally sized holes in the nose cone, which would open when an identical smaller cone on the inside would rotate. Four offset tubes would pass air through, causing the rocket to rotate about its vertical axis and convert energy to torque, thus slowing down the vehicle. This design was noted to pose significant issues, namely that this design was unlikely to significantly slow down the rocket, not satisfying the project objective. Furthermore, this design posed the risk of causing the rocket

to flip upon opening, as the centre of pressure would shift too far forwards to maintain stability.

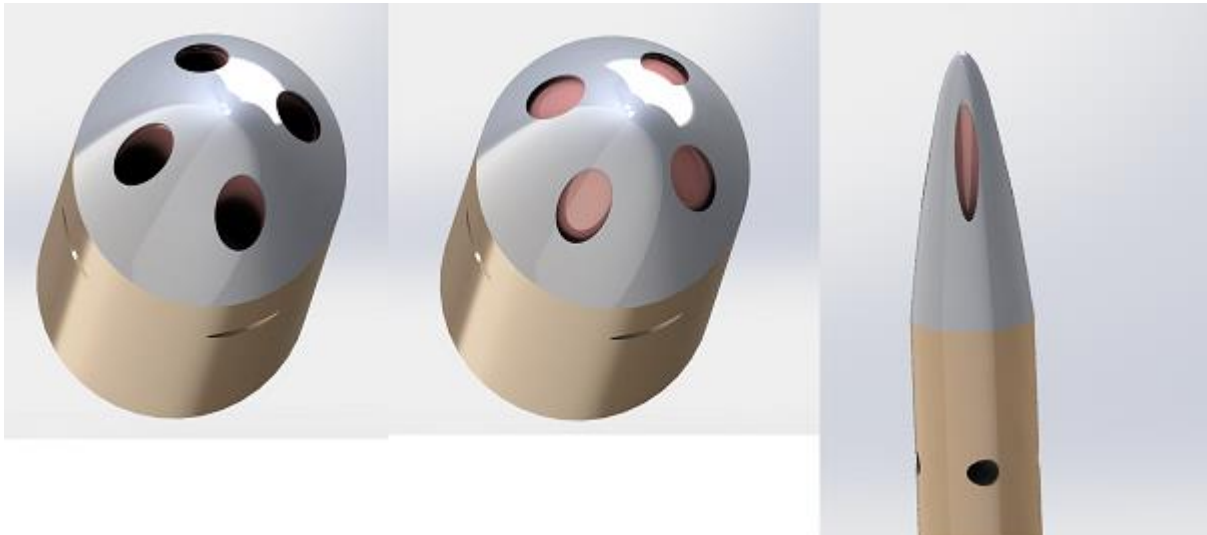


Figure 2.1: Holes in nose cone design

The second possible design, depicted in figure 2.2, was flaps that would radially deploy from the rocket body. A single servo would open the flaps, keep them open for the required two seconds, and then close them again.

This design proved advantageous, as the drag would be perpendicular to the flaps, the servo would not have to overcome any significant aerodynamic forces. This design allowed for altered angles at which the brakes would deploy.

However, due to the radial operation of the design, these brakes would have to be mounted above the fins, resulting in turbulence over the fins after deployment.



Figure 2.2: Radially deployed flaps design

The third design (depicted in figure 2.3) proposed three flaps to be placed between the frame and motor mount, with mechanically actuated cams to deploy and hold the brake panels open. Non linear cams allowed for a greater mechanical advantage the further the brakes deployed, and hence. Each cam would be attached to an actuator rod, which would move along a linear path due to a high torque servo positioned above the bulkhead.

This design allows for future use in altitude control, due to the ability to control the angle at which the flaps deploy. Pitch and yaw could also be controlled through differential deployment of each control surface. The design is compact, and able to be mounted low enough as to not cause major stability issues.

These brake panels would open directly into the free flow stream, however, posing the risk of snapping off if the downward force overcomes the adhesive forces used to secure the control surfaces to the hinges. Furthermore, the servo must be able to withstand deployment and overcome drag forces once extended. Due to the positioning of the servo, the black powder parachute deployment could not be used, and a separate ejection charge would be required.

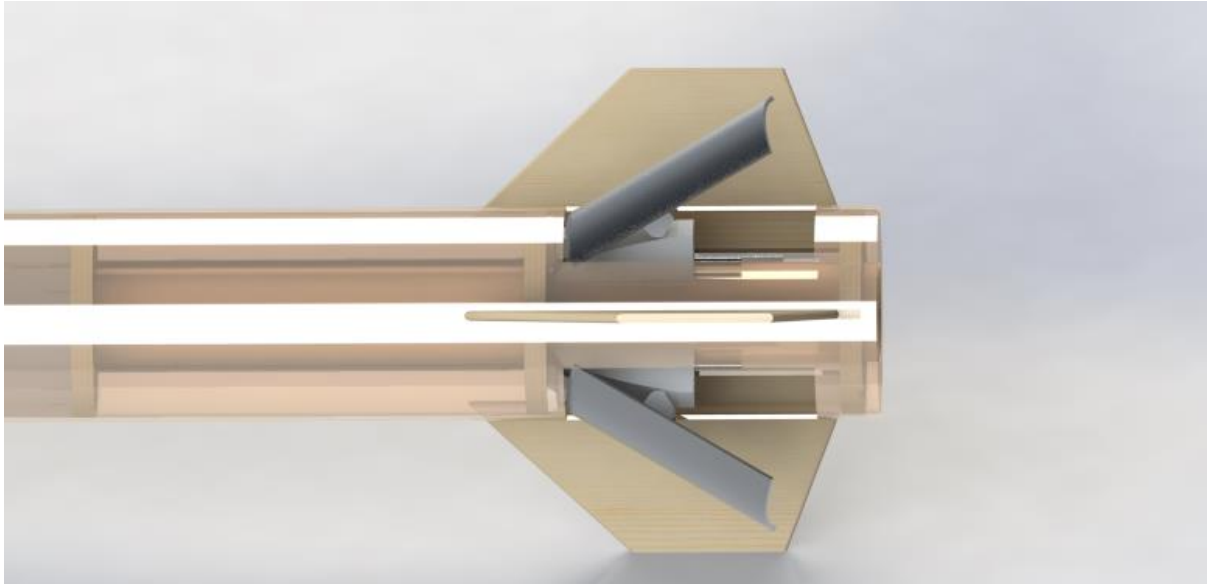


Figure 2.3: Flaps between fins design

All three designs were scrutinised in a decision making table in terms of the requirements from the OFFERS analysis. Each design was rated in terms of performance, aesthetics, safety, and cost. Design three, “Flaps between fins”, with the greatest deceleration force and lightest weight, was rated the highest of the three designs.

Therefore, “Flaps between fins” was chosen as the final design. The simplistic design offers a reliable method to decrease acceleration. With one of the project objectives being future use for HPR, this design would be easy to scale up to larger rockets, and with some modifications, offers the ability for yaw and pitch control, allowing for better more precise altitude targeting.

The remainder of this section covered design details, considerations and performance, simulations, and electronics.

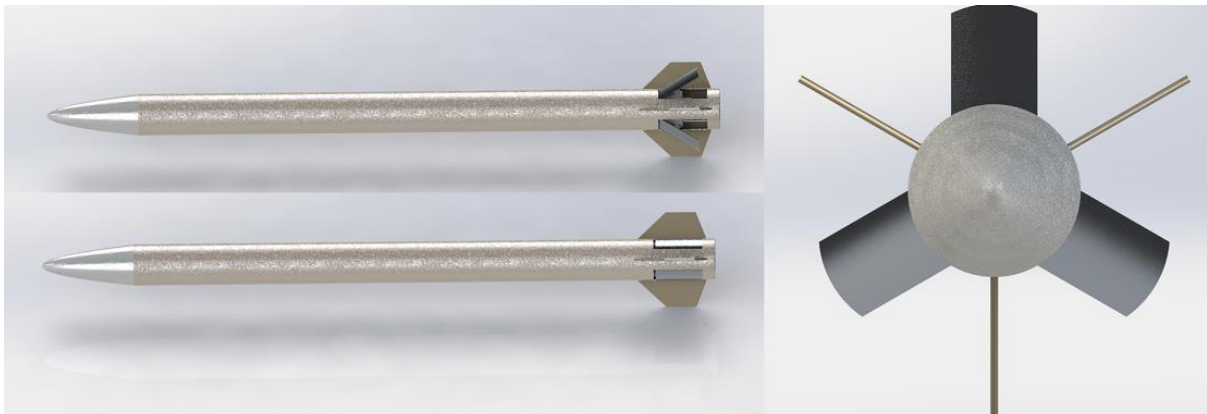


Figure 2.4: Final render of flaps between fins

The Gantt chart set a reasonable timeline in which to complete the project. Over the twelve week semester, a rocket with a functioning air braking mechanism had to be researched, designed, built, tested, and flown. Internal deadlines were set to keep the team on track and insure project completion by the end of the semester.

The report concluded on isometric drawings of all three possible designs, including further details of the final design. Appendices included an outline of required purchases, and drag calculations.

Section 3- Final Design:

3.1: Test Rocket Criteria

The design brief for this project specified that the designed airbrake system must satisfy each of the following criteria, when tested on an experimental rocket:

- Easy integration of a microprocessor able of controlled modulation of the control surfaces
- Design must have an *effector* for actuation of the brakes
- Must retract brakes after a predetermined time
- Simulation and effective implementation of an aerodynamic surface
- Fast actuation of the control surfaces <1.0seconds
- Remain open for ~2.0seconds
- Remain stable after actuation and not damage control surfaces whilst active

The chosen design to be outlined in the following sections satisfies all imposed design requirements.

3.2: Final Design

The final rocket design placed in the test rocket is summarised in the following sections.

3.2.1- Design Overview

The final fully assembled rocket is seen in figure 3.2.1.1 alongside an accurate cad representation. The rocket utilises a 65mm OD phenolic airframe paired with a 29mm H135W motor. The rocket has been designed with serviceability and reparability as a key factor during the design process. To achieve this the air braking mechanism along with the fincan and motor mount is entirely removable. This was chosen over methods of permanent fastening components- such as use of epoxy- so the mechanism can be adjusted and tuned easily. This enables the rocket to be easily repaired in the case of a component failure, and easily upgradable if desired.



Figure 3.2.1.1: Rocket versus CAD render

This design was chosen over other designs due to having the least penalising effect on the rockets stability when compared to the other designs initially proposed. The impacts the brakes have on stability is analysed using CFD (section 4.1) and suggests that minimal impacts were observed. This aligns with the observed stable trajectory of the rocket.



Figure 3.2.1.2: Disassembled rocket (left) fastening points (middle) motor thrust plate (right)

To disassemble the rocket, the screws in the red boxes are required to be removed, these are M3 hex panhead screws and interface with embedded M3 nuts in the centering rings. Wood screws are used to retain the thrust plate, made from a 5 thick laminate of 4mm plywood. These screws are responsible for connecting the motor thrust bulkhead to the airframe, along with the motor tube, centering rings and airbrake mechanism. Due to the fit between centering rings and the motor tube, the thrust from the motor was transmitted through the motor thrust bulkhead reducing loading off the sensitive fincan and brake mechanism centering rings which were made from 3D printed ABS.

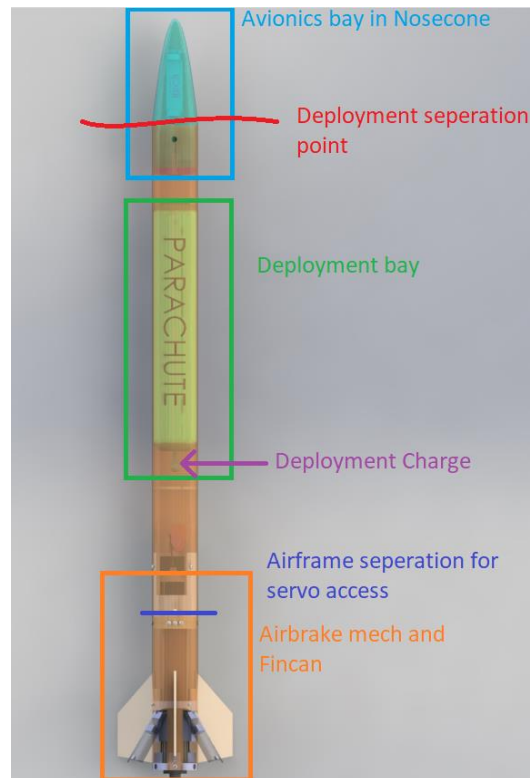


Figure 3.2.1.3: Internal structure of the rocket

Figure 3.2.1.3 shows the internal structure and layout of the rocket. At the top of the rocket is the nose cone seen in figure 3.2.1.4, which contains the avionics and data logging electronics (more detail in section 3.4). Below this is the deployment bay with the 24-inch parachute and the deployment charge. To separate the rocket a signal from the RRC3 altimeter is sent into the deployment charge. The deployment charge is made from the motor burnout ejection black powder and is wrapped up in tissue paper and masking tape. Using this deployment was necessary over motor burnout due to the servo actuation mechanism being directly above the motor ejection charge if it were installed.

The nose cone is a 150mm long parabolic nose, this was chosen for its greater performance at subsonic speeds [1] and large internal volume for avionics

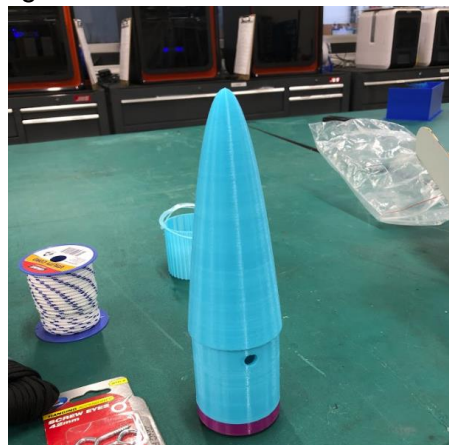


Figure 3.2.1.4: Parabolic nose cone

In the deployment bay is a single baffle plate epoxied in place. This serves to protect the servo and airbrake mechanism from the hot and corrosive black powder gasses. The baffle plate has a hole that allows the shock cord and wires to pass through to the servo.

The servo mount serves as the coupler between the forward and rear airframe, and allows for these two sections to be fastened using the same M3 screws as the fincan. The servo mount has the attachment point for the shock cord.

Below the servo mount is the fincan and air braking mechanism. (The air braking mechanism is detailed in section 2.1.2) The fincan seen in figure 3.2.5 is made from a section of the body tube and retains the epoxied fins in place. The cuts in the fincan for the air brakes were made using a dremel and a file.

The rocket was launched off a 1010 aluminium rail section, to accomplish this the rocket used two launch lugs. One launch lug was printed into the aft centering ring, this was required as launch lugs are needed near the rear of the rocket, and the launch lugs can not be epoxied onto the flaps. The top launch lug was installed at the centre of pressure and was also 3D printed and epoxied onto the airframe.

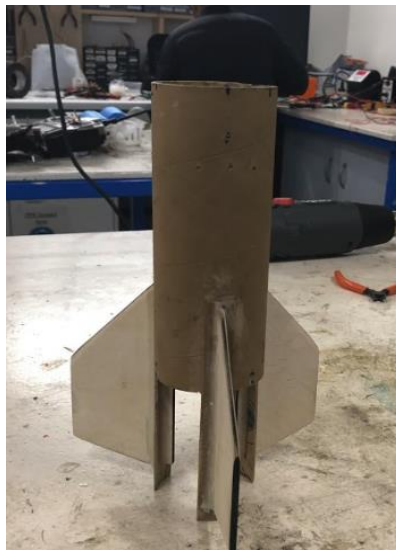


Figure 3.2.1.5: Fincan without airbrake mechanism installed

3.2.2: Changes from first submission

The core design described in the first submission remained the same, while details were altered and improved as the assembly came together and potential problems were identified.

The initial design had three equally sized gaps cut into the phenolic tubing, each the exact size of the brake panel. Therefore, when the brakes were in the retracted position, the rocket body exterior would have minimal drag.

Once the prototype was constructed, it became evident that the brake panels would not be able to deploy and retract without catching on the edge of the phenolic body frame.

To compensate for the field of movement of the panels, the gaps were cut around half a centimeter longer along the vertical axis. CFD analysis showed that the boundary layer around the brake panels was sufficiently large, so that the gaps would not pose an issue.

The shape of the cams has been altered since the preliminary design. Both the cam and the brake panel attachment have been redesigned to slide over each other without the possibility of the upper component displacing.

To prevent the cam itself displacing, two extra steel rods were inserted into the lower centering ring. This restricts the cam's movement to a strict linear path. These alterations can be seen in figure 3.2.2.1

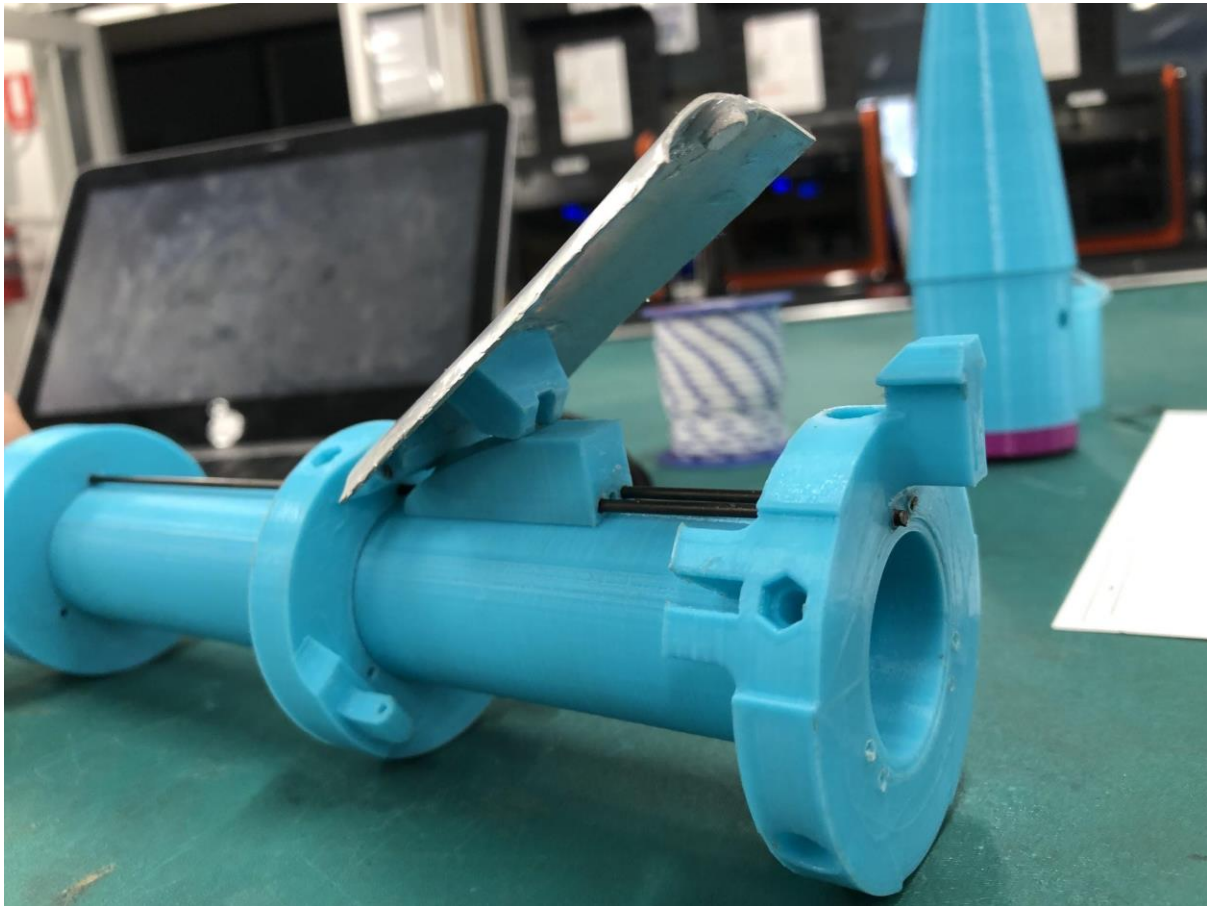


Figure 3.2.2.2: Prototype of the cammed mechanism

For ease of access and repair, the entire actuation mechanism was made removable. Rather than permanently attaching the braking mechanism to the inside of the rocket body, screws and bolts held the lower rocket components together. The rocket separated above the fins, with the servo mount acting as a coupler.

3.2.3: Mechanical actuation system:

The mechanical actuation system utilised is based off a rotational servo as the effector seen in figure 3.2.3.1. Choosing a servo simplified the overall mechanical system, as the servo allows for direct programming of an actuation angle and requires minimal calibration. Contrasting this to a design using a dc motor with a rack and pinion type design, it is very

much harder to determine the actuation angle of the flap without extra sensors onboard increasing complexity. Stepper motors and linear actuators were not fast actuating and not able to fit the strict volume and weight limits in the rocket. That leaves the servo as the ideal choice for this application.



Figure 3.2.3.1: Servo connected to actuator piston (left) Actuator piston with servo linkage (middle) Assembled and powdered air brake mechanism (right)

The flaps are controlled and operated, using the servo. When the signal from the microcontroller arrives to the servo it specifies the servo rotates 120 degrees clockwise from its current position. This pulls up on the actuator piston. As the actuator piston is connected to all 3, 2mm steel actuator rods, this then pulls those upwards also. The cams (seen in figure 3.2.3.2) are directly connected to the actuator rods and move upwards, increasing pressure on the cam followers on the flaps. This causes the flaps to open outwards and into the airflow, slowing the rocket.



Figure 3.2.3.2: Flap actuation mechanism

To ensure that the cams remain in a purely vertical direction, each cam has two 2mm steel guide rods installed. The cams also have a ridge running the length of travel. This matches a

slot in the cam followers and reduces the sideways play in the flaps seen in figure 3.2.3.3. To ensure that the flaps close after the servo retracts, 2 neodymium magnets are used per flap. One of these magnets is epoxied to the flap and the other to a recessed hole in the aft centering ring.

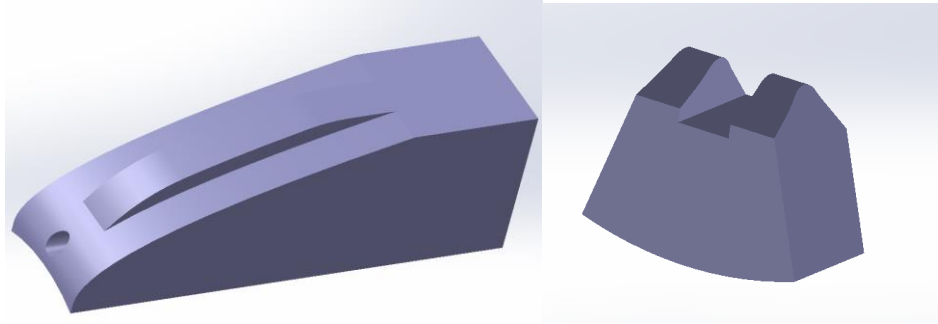


Figure 3.2.3.3: Cam (left) Follower (right)

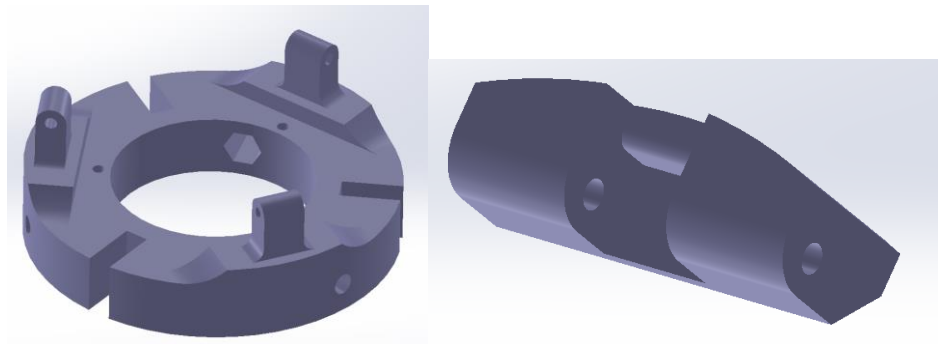


Figure 3.2.3.4: Flap hinge mechanism

The flaps are connected to the top centering ring mounted to the motor mount using the hinge system seen in figure 3.2.3.4. This allows for the two parts to interface, and a section of 2mm steel rod is used as a pin to hold them together. The notches in the centering ring are there to allow for the fin tabs to slide past when the mechanism is installed/removed. A similar notch is used on the aft centering ring to ensure that the fin tab remains in the centering ring fin slot. All these components fit together as a functional assembly and behave as expected. The assembly with the brakes in the opened and closed position is seen in figure 3.2.3.5.

Due to the complexity of the parts used in the mechanism, it was necessary that they be 3d printed as this level of detail is easily accomplished. To reduce thermal issues from the motor burning, all mechanism parts are printed using ABS due to its superior thermal resistance. The linkage arm that connects the servo to the actuator piston was made from bent 2.5mm steel wire and its length adjusted so that the correct throw of the servo was obtained.

Due to body frame diameter restrictions and the size of the servo, the largest possible servo arm is 20mm, the servo arm was ground down using a dremel to ensure that it fitted clearly

into the airframe. Using a 20mm servo arm this provided 35mm of vertical travel of the cams over the full 120 degrees of servo actuation.

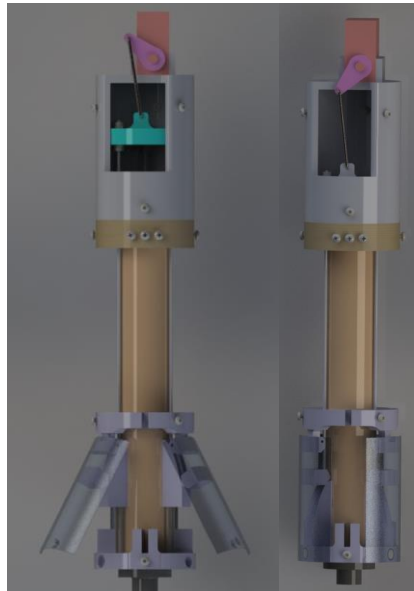


Figure 3.2.3.5: Braking mechanism open (left) closed (right)

During the optimisation process of the cammed flap mechanism, it was noted that the application of the aerodynamic drag forces on each flap increase with the angle of actuation of the flap. This would mean higher stresses on the servo and potential for the mechanism to not fully deploy. To mitigate this problem the cam was designed to have a non linear profile, where at higher angle of actuations the servo has a higher mechanical advantage. This can be visualized in figure 3.2.3.6. The chosen profile was parabolic, with a lower mechanical advantage at low actuation angles.

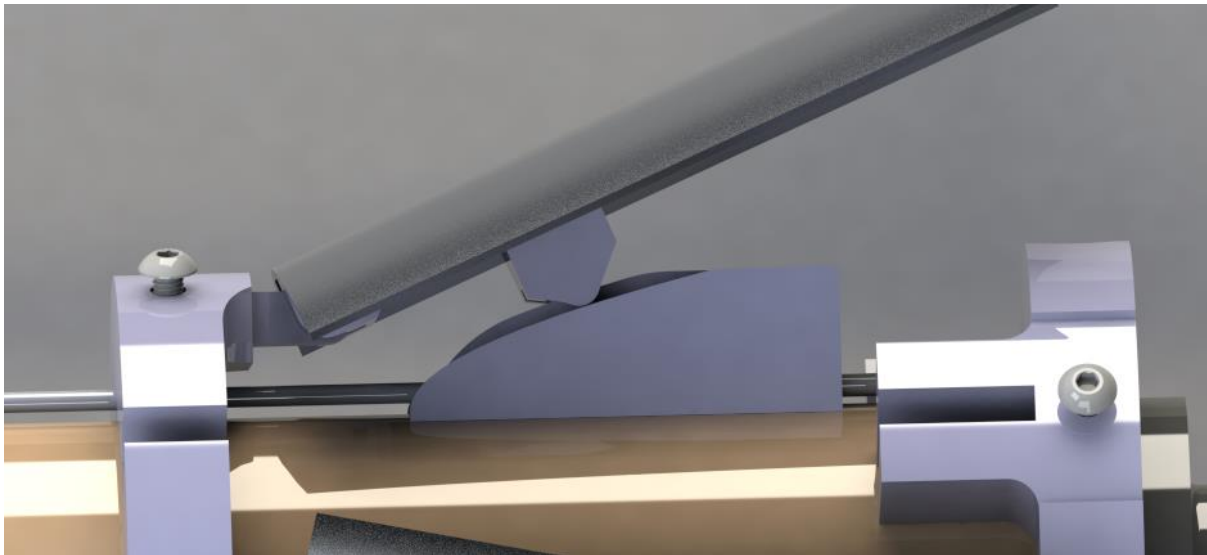


Figure 3.2.3.6: Close up of nonlinear parabolic cam and follower mechanism

By knowing the actuation angle of the servo and the profile of the cam, this allows for the flap actuation angle to be plotted as a function of the servo actuation angle, this could be used by a microcontroller to specify the actuation angle of the flaps, allowing for custom modulation. By relating the relative angle change of the servo compared to the flap, an effective torque factor can be determined also as a function of the input actuation angle.

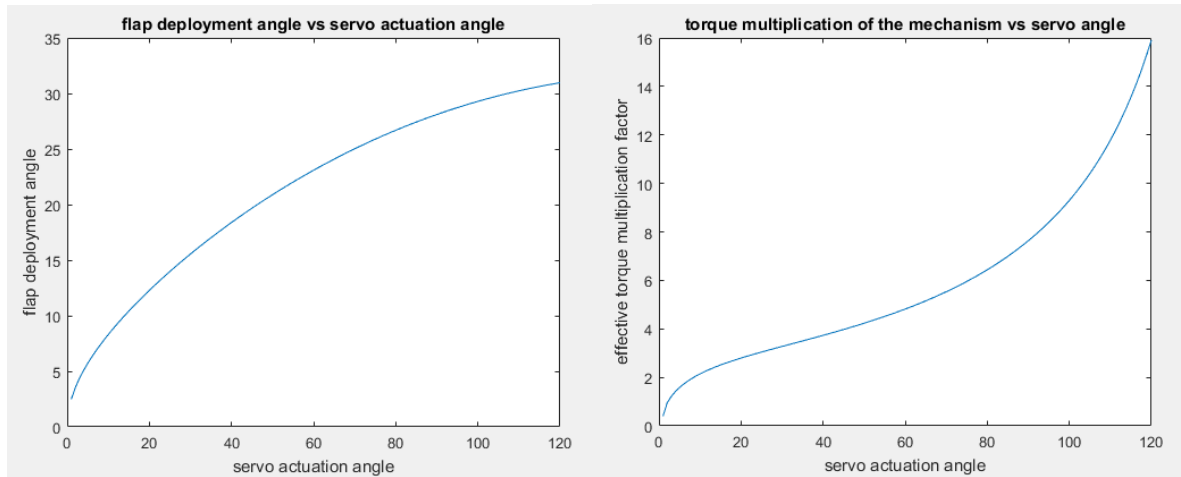


Figure 3.2.3.7: Flap actuation and effective torque multiplication as a function of servo actuation

Due to the sine component from the rotary to reciprocatory motion of the servo and actuator piston, the torque multiplication factor is a product of the sine and parabolic components. This design allows for modulatable flap actuation from 0-30 degrees.

To ensure that the flaps will not detach during flight, each of the 3 flaps were opened to their 30 degree open position and loaded with 1.6kg on the tip of the flaps, this was above the expected loading at the time of 15N based on preliminary flap plate drag calculations. The load was also offset from the pivot further than the expected centre of pressure on the flaps leading to a higher safety factor.

3.3- Rocket Avionics Systems:

3.3.1- Hardware

Below is a block diagram summarising the avionics systems aboard the test rocket.

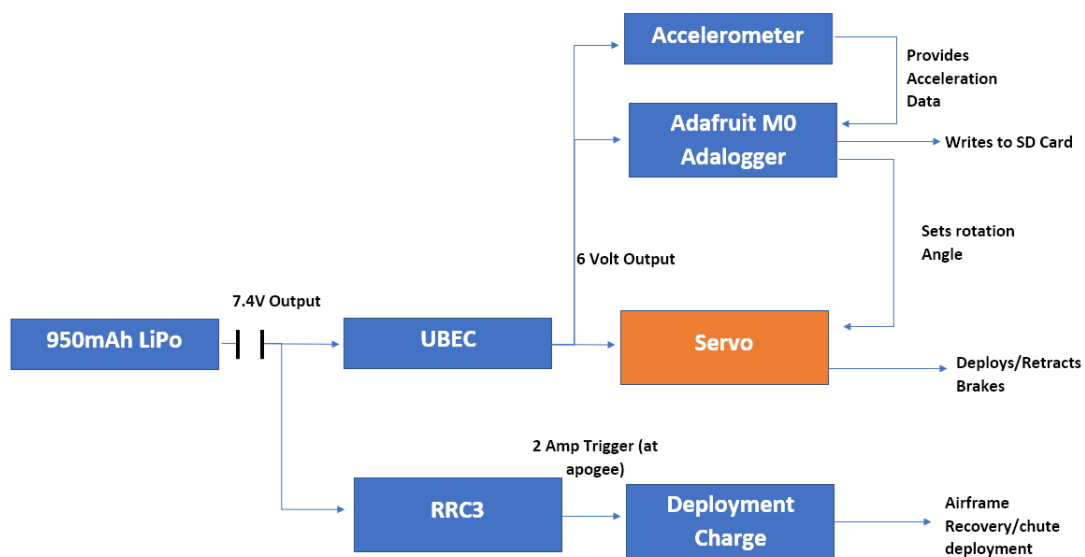


Figure 3.3.1.1- A block diagram illustrating the overall system architecture of the test payload, and recovery system.

The system was powered using a 950 mAh Lithium Polymer (LiPo) battery, which had a voltage output ranging between 7.5 - 8V. This power source was chosen based on its high capacity and rechargeability. Though the electronics used in the system had a very low power consumption, to ensure there was no unnecessary reliance on constantly charging the LiPo before testing sessions, a larger capacity unit was chosen for use.

The whole system was armed using a single-throw-double-pole switch, which was connected in series with the LiPo. This switch served as a fundamental safety feature in the design as it prevented false ignition of the deployment charge while the vehicle was still being prepared on the ground, and also potential for the false activation of the air brakes when not testing- unnecessarily deploying the breaks could increase the risk of damage to the actuation system.

The output from the LiPo was stepped down using a UBEC buck converter. This component stepped-down the voltage to 6 volts, which was the optimum operating voltage for the servo selected to deploy the control surfaces. The six volt output from the UBEC was then transferred to the other components of the system.

The Adafruit Adalogger was used as the primary processing unit for the system. Its selection was largely due to the presence of an onboard SD card slot, which could read and write data to the chip. If another board had been used, a separate SD-card adaptor would have needed to be included in the design, likely slowing the system down and also increasing mass. As the accelerometer recorded the acceleration of the vehicle, the adalogger analysed this data to ascertain whether the motor has ignited, and also wrote the data to the SD card.

The accelerometer used (the Adafruit LIS3DH) was connected to the adalogger in the I2C connection format [2]. This data transfer format was utilised as it generally allows for less noisy (albeit slower) data transmission. The accelerometer was chosen based on its high G-force rating (can compute acceleration up to 16Gs). The data output from this sensor was also remarkably stable, with very little apparent noise when measuring on the ground, suiting it to collect data for the test flight.

The servo chosen for use in the system was the *TrackStar TS-910* which was capable of generating up to 3Nm of torque. This meant the component was well suited for the high drag force it would need to overcome when deploying the air brakes which was approximated around 10N based on CFD.

The avionics sled was manufactured out of 3mm plywood. The material was laser cut to match the shape and profile of the nose cone, in order to ensure it was not loose during flight (having it move around in the nose cone could serve to destabilise the rocket as it flew). The image below shows the AV sled while still under construction:

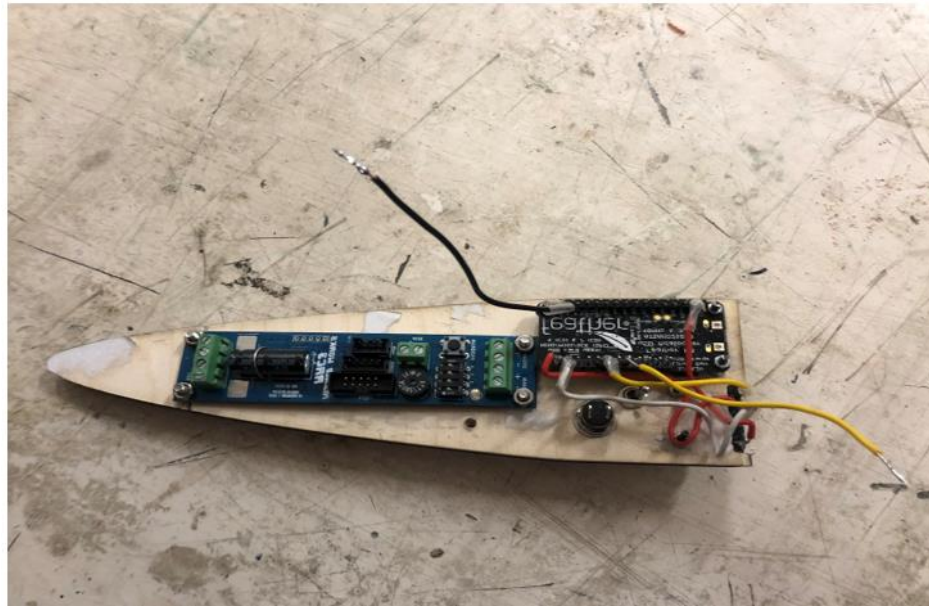


Figure 3.3.1.2- An image of the AV sled while still being prepared for flight.

The components were secured onto the sled using M3 bolts. To fit all components, the adafruit adalogger and RRC3 were mounted on one side of the sled, while the accelerometer, LiPo, UBEC and switch were mounted on the opposite side of the sled.

All electrical connections in avionics bay were soldered, with insulation tape or heat shrink applied over the joint to minimise the risk of short circuits. To secure the LiPo and UBEC in place, insulation tape was wound around them and around the edge of the sled.

3.3.2- Software

In accordance with the design brief, the test rocket was required to deploy air brakes at burnout off the chosen motor. The brakes were to be extended over a period of 2 seconds, before being retracted.

The first design consideration the team had to make, was how the avionics systems should “detect” burnout, in order to deploy the brakes. A valid method of doing this could be using the accelerometer included onboard. Once the motor fuel was exhausted, the thrust accelerating the rocket would no longer be present. As such, rather than having a positive acceleration (taking the positive direction as away from the ground), the net acceleration would be due to drag and gravity, and as such the acceleration would become negative.

Initially, it was planned for the brakes to deploy once a negative acceleration was detected by the accelerometer. This approach, however, had a fundamental limitation. Firstly, it was not possible to fully test the system under the conditions it would operate under during flight. Most of the other facets of the rocket, such as the servo’s rotation and actuation of the brakes could be rigorously tested on the ground before flight, ensuring any possible issues could be rectified. In the case of detecting burnout using the accelerometer, however, there

was no means of simulating the noise in acceleration of the rocket- which could be more evident as the rocket would be flying at a very low altitude at burnout. This could mean the brakes may deploy too early while the rocket is still accelerating, potentially causing damage to the actuation systems, if the accelerometer readings were particularly noisy during flight.

Instead, to allow the system to detect burnout the published burntime of the motor, provided by the manufacturer, was utilized. The motor used had a predicted burn time of 1.9 seconds. This value is prone to mild fluctuations based on the conditions the motor is burnt under, as well as manufacturing tolerances, and the motor may burn for slightly more or slightly less time than it is rated to. To ensure the brakes deployed slightly after burnout, the program controlling the actuation system timed 2.2 seconds from ignition of the motor before sending a signal to the servo..

In order to detect ignition of the motor, which would start the aforementioned countdown till brake deployment, acceleration data was monitored for large spikes in the G-force experienced by the rocket. Immediately following ignition of the motor, the rocket is exposed to large accelerative forces. The test rocket the brakes were incorporated into was simulated to experience up to ten times the force of gravity (Gs) while the motor was burning. As such, to detect ignition of the motor, the program checked acceleration data for absolute values exceeding 2.5Gs in the Y-axis (relative to the accelerometer). Given the configuration of the avionics bay, the positive Y direction programmed into the accelerometer was pointing out of the nose cone, perpendicular to the ground when the rocket was placed on the launch rail. To prevent accidental bumps from triggering the count down, the program stored acceleration data over a period of 20ms, and after finding the average of the data, ensured the countdown only began if the acceleration exceeding 2.5Gs was maintained over a period of time.

Once the timer reached 2.2 seconds following motor ignition, a signal was sent to the servo, in order for it to rotate to an angle of 110 degrees. This angle was selected, as during testing it correlated with a full deployment of the brakes to an angle of approximately 30 degrees. In testing, the servo took approximately 0.5 seconds to fully open or close. For this reason, signals to open and close the servo were sent 3 seconds apart, so the brakes would be in their fully deployed configuration for 2 seconds, as was stipulated in the project brief.

Lastly, to analyse the efficacy of the air brake system employed, the accelerometer data had to be stored in some form so it could be analysed once the rocket was recovered. To make this process easier, the Adafruit M0 Adalogger was employed as the primary processing unit for the avionics system. As mentioned earlier, this board has an in-built SD card slot with the ability to read and write data to the storage devices. The system was programmed to store acceleration data into a .txt file aboard the SD card at a rate of 100 Hz. As the process of writing to a storage device is quite computationally intensive however, the device was only capable of writing data at rate of 44Hz. The format of the data written is summarised in figure 3.3.2.1:

1.15	-89.09	2.41		-2.07	12.53	1.15	NDAB
1.61	-98.63	0.34		-2.18	12.64	0.80	NDAB
-4.60	-92.42	0.11	NDAB	-2.18	11.95	1.03	DAB
-4.02	-89.66	-2.53	NDAB	-1.49	12.07	1.38	DAB
-3.10	-101.96	3.10	NDAB	-1.84	11.95	1.38	DAB
-1.38	-115.87	1.72	NDAB	-1.61	12.30	0.69	DAB
-2.53	-114.83	2.87	NDAB	-1.03	11.84	1.61	DAB
-4.14	-108.05	1.03	NDAB	-0.46	12.30	1.26	DAB
-5.06	-112.65	3.68	NDAB	0.00	13.45	1.03	DAB
-3.22	-119.89	2.53	NDAB	-0.23	13.91	0.57	DAB
-4.14	-110.01	-0.34	NDAB	0.00	15.40	0.23	DAB
-3.56	-116.10	1.15	NDAB	0.11	16.44	0.46	DAB
-3.45	-115.52	0.23	NDAB	0.34	17.70	1.38	DAB
-2.99	-112.42	0.80	NDAB	0.00	18.85	0.23	DAB
-5.06	-113.80	1.95	NDAB	-0.23	19.89	0.46	DAB
-4.37	-114.95	0.69	NDAB	-1.03	20.35	-0.34	DAB
-3.56	-118.51	0.92	NDAB	-0.69	20.58	0.00	DAB

Figure 3.3.2.1- Image illustrating how data was written to the SD card. Once motor ignition is detected, the status of the airbrakes is set to NDAB (Not Deployed Air Brakes). After the 2.2 second timer, the status is set to DAB (deployed air brakes) while the flaps are deployed.

Section 4- Design Performance:

4.1- Simulated Performance:

To assess the veracity of the test flight results, the performance of the air brake system was simulated using *SolidWorks Flow Simulation*. The assembly of the rocket, with all non-essential parts inside the airframe like bulkheads, and mounts were removed. Figure 4.1.1 illustrates the overall model used in analysis:

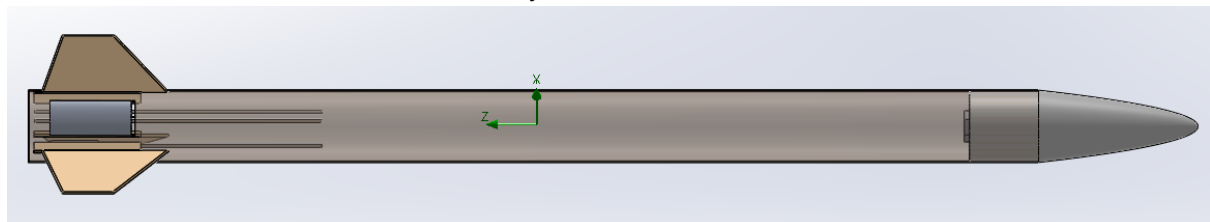


Figure 4.1.1- The model used for CFD analysis- all unnecessary internal components were removed during analysis. The thread rods connected to the cams were maintained, however, to ensure the flap angles set during analysis replicate those during flight.

The first goal of the CFD analysis was to analyse the drag induced by deployment of the air brakes. In order to do this, two test cases were run- one where the brakes were deployed to their full deployment angle of 30 degrees, and another where they were fully retracted within the air frame. The parameters set for these analyses is summarised in table 3.1:

Table 4.1.1- Summary of the parameters surrounding CFD analysis. Note that the fluid flow was a linear stream of air travelling from the nose cone to the base of the rocket, hence simulating air flow as the rocket is travelling through the atmosphere.

Fluid Type	Fluid Flow Rate	Flow Type	Temperature	Pressure	Surface Finish (Roughness)
Air	126m/s	Laminar/Turbulent	293.2 K	95460.84 Pa	100 micrometres

A flow rate of 126 m/s for the air was selected as it was the experimentally determined maximum velocity the brakes were exposed to. Furthermore, the pressure selected was that at an altitude of approximately 500m, when the brakes deployed.

The meshes used for the two test cases are provided in figure 4.1.2. As the areas with the most interesting flow characteristics were near the front (over the nose cone) and rear (over the breaks and fins) of the vehicle, the mesh was adjusted to have the greatest resolution in these areas. The case where the brakes were retracted had fewer mesh elements as it lacked deployed air brakes. To analyse flow over and around air brakes to a high degree of precision, more mesh elements were required. In all, the case with retracted breaks had approximately 500,000 mesh elements, while the case with deployed breaks had around 1.3 million.

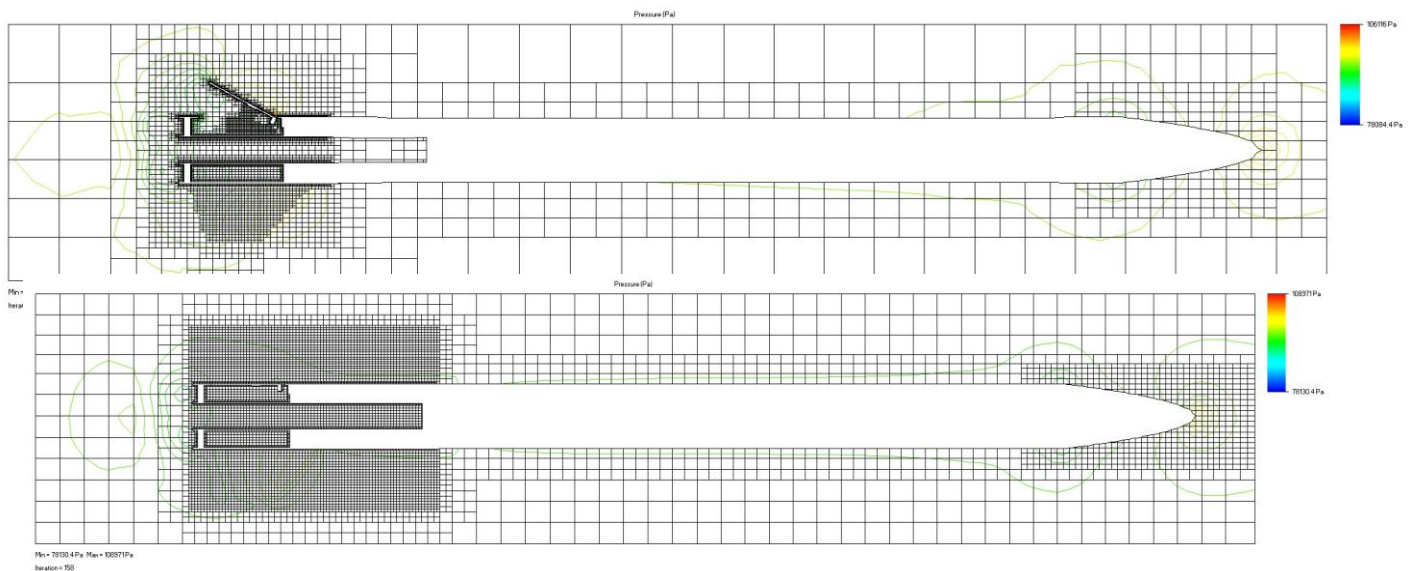


Figure 4.1.2- Pressure plots of the two test cases with the meshes used for analysis included.

To ensure results could be compared for the two test cases, all parameters regarding the CFD were kept constant, save the deployment status of the air brakes. To ascertain the net drag caused by the deployment of the air brakes, the total drag of the models used in the two cases was found, and the difference between these values assumed to be caused by the control surfaces. Table 3.1.2 summarizes the net drag of the two test cases.

Table 4.1.2- Net drag of vehicle with and without brakes deployed.

	Net Vehicle Drag (N)	Drag Due to Brakes (N)
Airbrakes Deployed	50	21
Airbrakes Retracted	21	>1

These simulated results indicate that there should be an increase in drag by a factor of approximately 2.4x when the brakes deploy. The data taken from the test rocket supports this assertion, as it was found that drag increased by a factor of 2.3x once brakes deployed. The drag values, however, seem to be overestimates of the actual drag force experienced

by the rocket during flight. Possible causes for this could be use of a coarse mesh or the lack of fillets around the fins modelled in the assembly. Inclusion of fillets in the simulated model would decrease the drag caused by air flow through the joints between the fins and the airframe. Beyond this of course, there is likely to be a degree of error in the experimental results, which can be .

The design brief stipulated that inclusion of the brake system on the vehicle should not adversely affect its stability. This led to the second part of the simulation analysis of the rocket, pertaining to the effects of the braking system on the efficiency of the fins on board the rocket. To perform this analysis, air at 126m/s was sent at a 10 degree angle of attack from the axis acting directly down the airframe. The aim of the analysis was to determine whether there were any substantial effects on the forces acting on the fins when the rocket presented with a substantial angle of attack. The results use a key provided in figure 4.1.3, with distinct names for each of the fin surfaces.

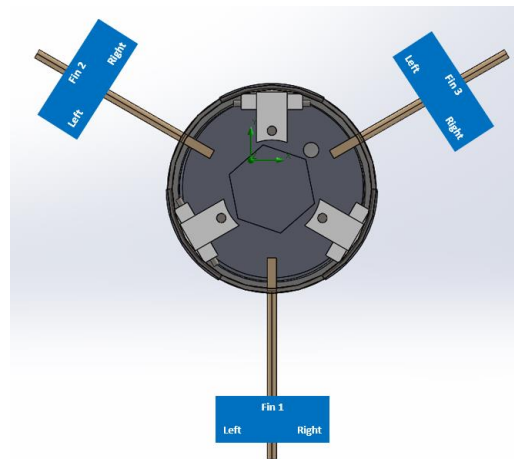


Figure 4.1.3- A key explaining the names of the different fins surfaces.

The results of the analysis are summarised in table 4.1.3.

Table 4.1.3- Summary of the forces applied on each fin surface, when brakes are deployed/not deployed.

	Airbrakes Deployed Test Case	Airbrakes Retracted Test Case
Fin 1 Left (N)	3.54	2.43
Fin 1 Right (N)	16.36	14.76
Fin 2 Left (N)	3.75	1.28
Fin 2 Right (N)	11.82	8.25
Fin 3 Left (N)	7.77	1.73
Fin 3 Right (N)	10.25	7.70

From these results, it appears as though almost all fins have an increased forces applied on them when brakes are deployed, compared when they are retracted. A possible reason for this could be the increase turbulence and vortex shedding from the top of the brake panels, as well as increased velocity of air as it passes over the brakes, which would be impacting upon the fins.

Once concerning finding was the substantially increased force acting on the left face of fin 3. This was likely due to the increased velocity of the air flow over the brakes which then directly collided with the fin, this phenomenon is illustrated in 4.1.4 (bottom) where air

travelling over the tips of the brakes appears to be travelling at up to 180m/s. Overall, however, there appear to be corrective forces applying on the breaks in both conditions, and as such the fins appear to be functioning as expected- hence suggesting little effect on the stability through placement of the breaks at the rear of the vehicle. Another metric for stability, the stability calibre was also considered, when designing the rocket, and the final design had a value of 1.71 at lift-off, which is well between the range of 1-2 where rockets are considered most stable

Figure 4.1.4 illustrates the flow of air over the airframe with a 10 degree angle of attack, as was simulated. In the lower image, a more in depth description of the flow can be observed, in figure 4.1.4 (bottom).

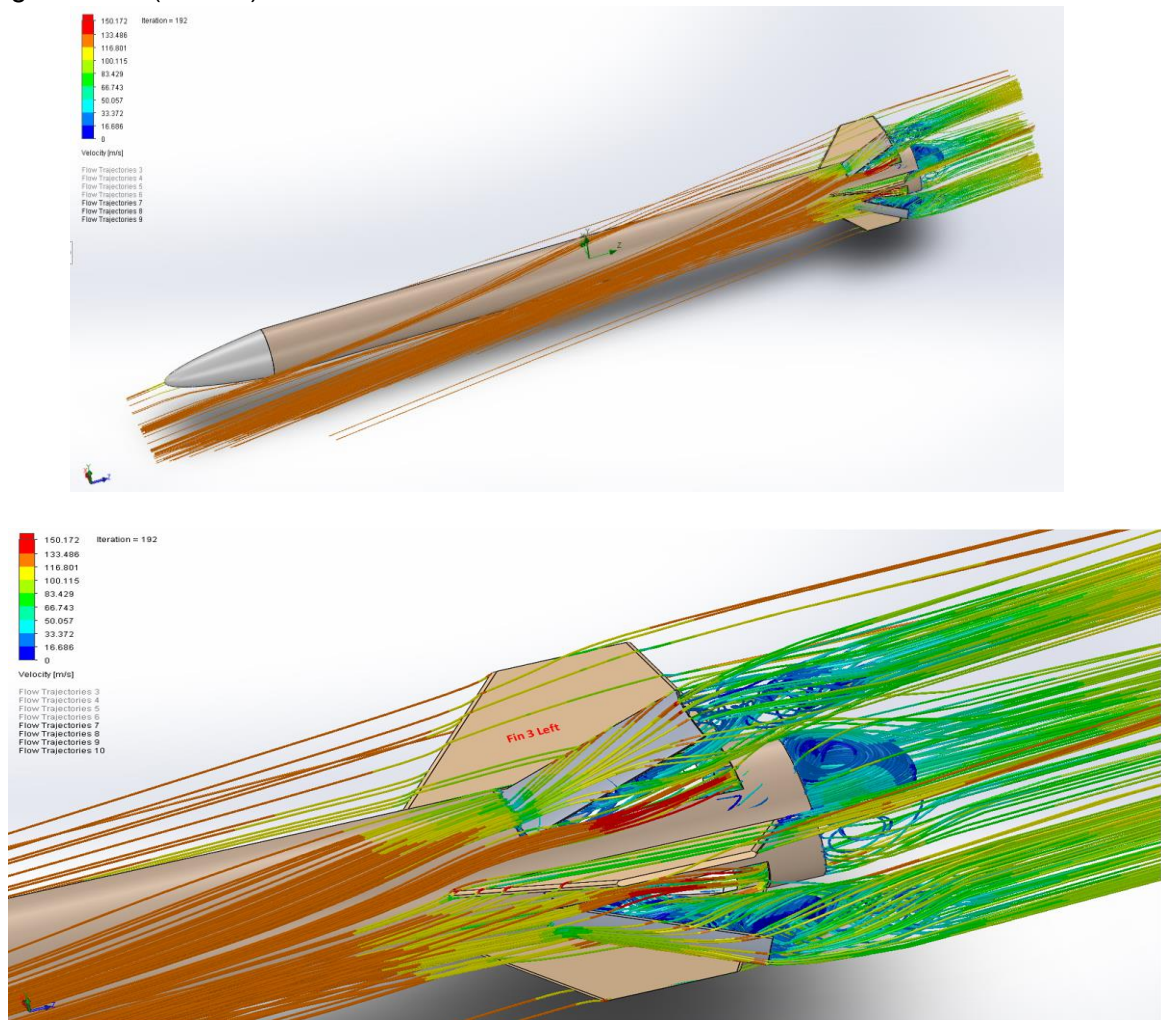


Figure 4.1.4- Illustrations of the air flow over deployed brakes when at a 10° angle of attack.

To get an altitude estimation without the air brakes opening, open rocket was utilised to analyse the performance of the rocket. This provides a valuable data set to compare the experimental collected data with the closed brake rocket. Ideally the rocket would be flown again with the same motor configuration but the brakes inactive and compared to the rocket with the brakes active however due to time constraints and costs this was not done. The simulated apogee was 805m or 2640ft.

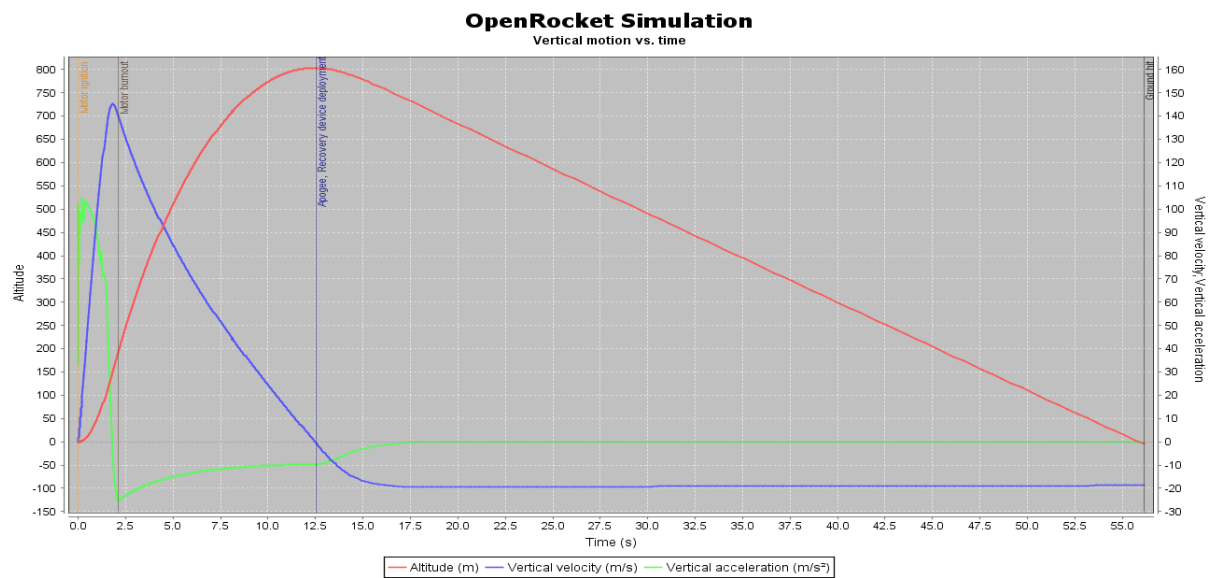


Figure 4.1.5: Open rocket simulation with the brakes closed.

4.2: Flight performance

Table 4.2.1: Open rocket simulated parameters

Overall Length	1060mm
Lift off mass	1325g
Stability caliber at launch	1.71 Cal
Max velocity	M0.42
Max acceleration	10.8G
Motor	H135W
Burn time	1.9sec
Thrust (Peak,Average)	160N, 116N
Impulse	229Ns

The experimental launch of the rocket carrying the air brakes was conducting on the morning of the 18th of May, at Drouin Airfield. Following set-up of the rocket, and its approval from the range safety officers (RSOs), the vehicle was racked onto the Melbourne Amateur Rocketry Societys' 2 meter long 1010 launch rail, in preparation for flight.

The rocket launched without issue, however, immediately following ignition, and as it cleared the end of the launch rail the rocket pitched on a slight angle. It successfully self corrected due to the rockets high stability margin at launch of >1.7 cal the rocket continued on a straight path until apogee. The parachute deployed as expected.



Figure 4.2.1: Rocket's initial trajectory off the rail, seen with minor slipping.

High decent velocity resulted in a rough landing. Furthermore, the magnets did not provide sufficient force to keep the brake panels closed upon decent. This combination were the most likely reasons as to why a brake panel broke off during landing. Upon closer inspection, this was determined to be an issue with adhesion, and not design.

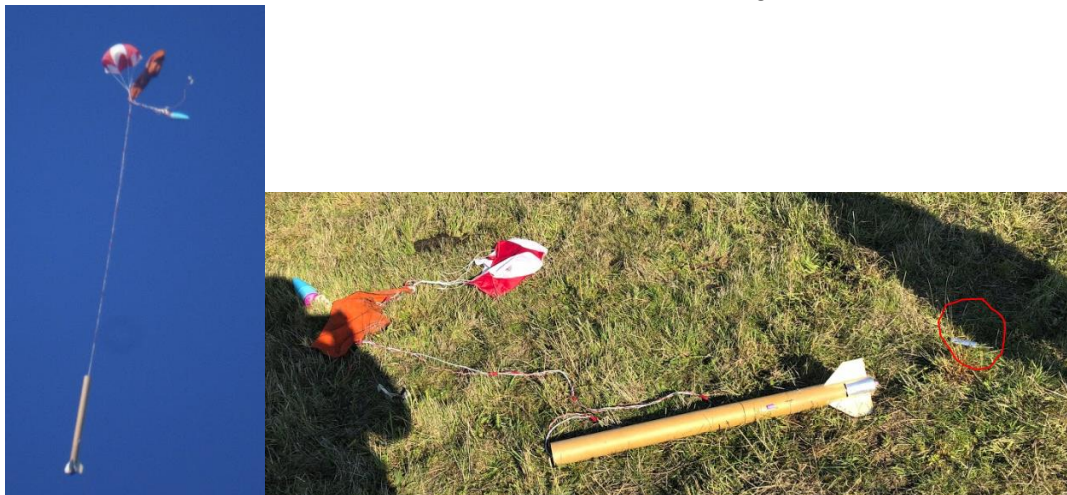


Figure 4.2.2: Rocket under descent (left) rocket on ground with detached flap circled in red (right)

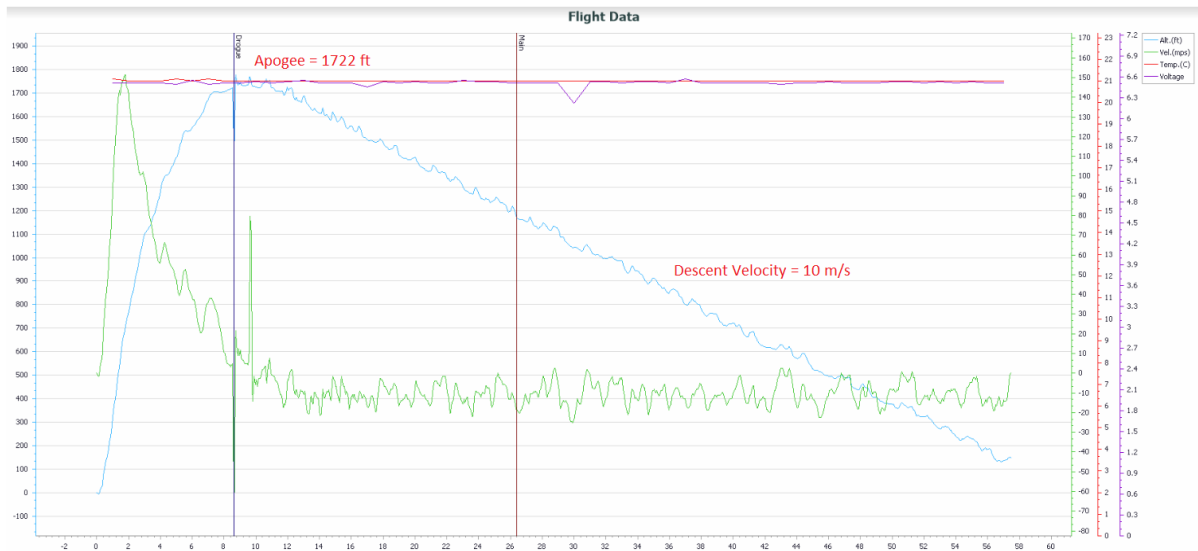


Figure 4.2.3: Altimeter plot from RRC3

The data retrieved off the RRC3 altimeter shows that apogee was experimentally measured to be 1722ft, comparing to the simulated 2640ft of the closed brake open rocket simulation this shows a reduction in altitude of greater than 900ft, reducing the altitude by over one third. This shows that the air brakes functioned as intended and reduced a substantial amount of altitude.

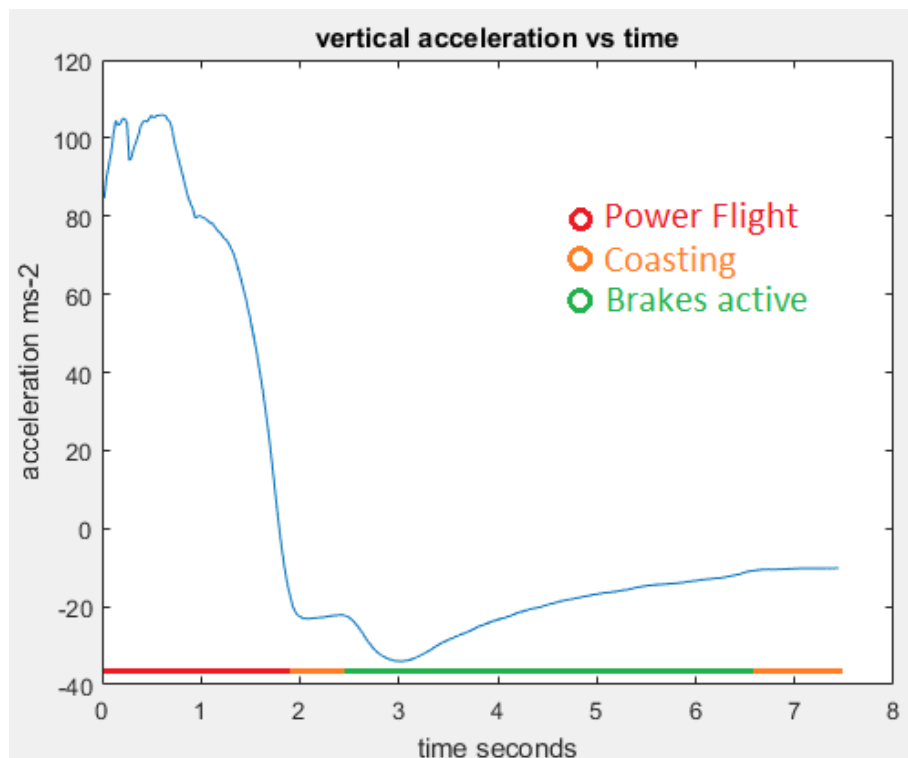


Figure 4.2.4: Vertical acceleration of rocket vs time

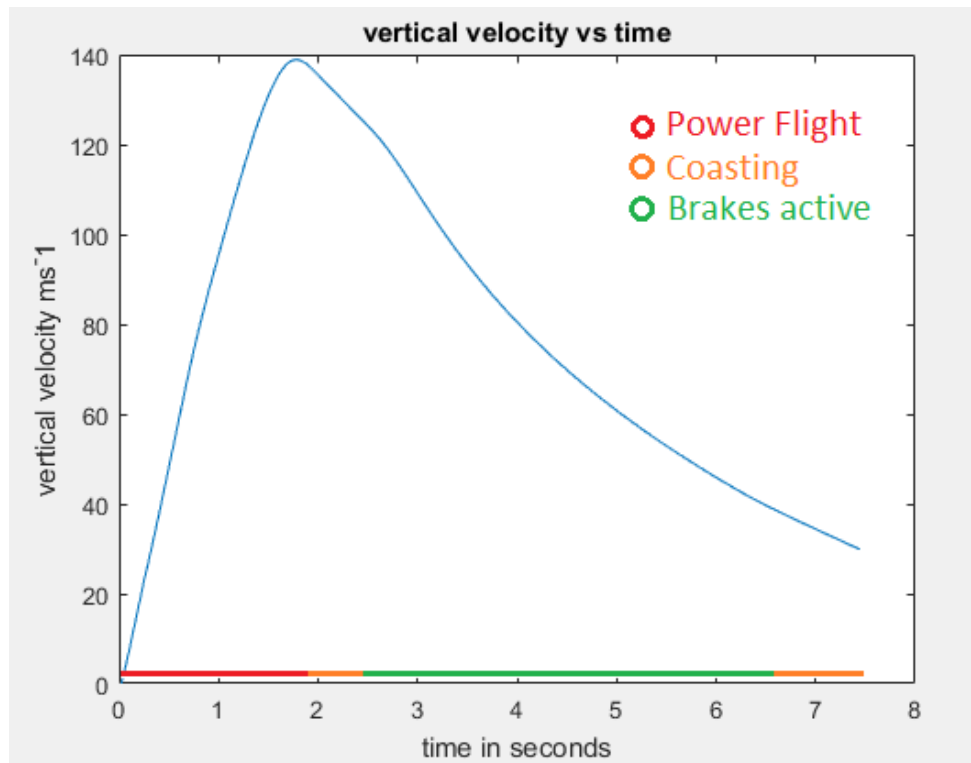


Figure 4.2.5: Vertical acceleration of rocket vs time

The vertical acceleration plot obtained from the onboard accelerometer shows effective operation of the air brakes. This is evident by the sudden increase in deceleration at 3 seconds into the flight. To analyse how much drag the air brakes added to the rocket, the total drag of the rocket needs to be compared before and after the brakes open. This can be done simply using $F = ma$, where a is the drag component of acceleration and m is the burnout mass of the rocket.

By taking the the difference in total drag from the point at 2.5 seconds to 3 seconds shows a change in drag from 13.3N to 30.1N, an increase by a factor of 2.3. It should be noted that this method has some error in analysis, this is due to the velocity changing between the two points as the breaks open from fully closed to fully open, this can be normalised by taking the determining the C_d of the rocket at each point, using the velocity at that point in time.

$$C_d = \frac{2ma}{\rho v^2 A}$$

To compare the changing drag of the rocket, assume the area of the rocket remains the same. Take breaks closed as $C_d = 1$ (normalised for closed)

Table 4.2.1: Normalised Experimental C_d of air brakes

	Ma (drag force) N	Vel (figure 3.2.5) m/s	C_d
Breaks closed	13.3	120	1.00
Breaks open 100%	30.1	98	3.39

The accelerometer data shows an effective increase in drag of 2.3x, however when normalising for the change in velocity at the instant that the brakes are open vs closed, this shows an effective increase in drag of 3.39 if the breaks are exposed to the same air flow velocity.

Due to the shape of the vertical velocity plot, at apogee the rocket is showing an apparent velocity of 30 m/s. This is due to the vertical component of acceleration and velocity being taken through the nose of the rocket, due to the mounting of the accelerometer. This suggests at apogee the rocket had a weather vane component of velocity of up to 30 m/s. This may have an unknown impact on the overall altitude of the rocket due to a change trajectory when compared to open rocket.

Incidents of Failure

The first major setback was uncovered upon receiving the servo, where the mechanism was found to rotate approximately 120 degrees rather than the 180 it was assumed to. As there was nowhere on the website the specified the rotation angle of the servo, it was assumed it would rotate to 180 degrees as most servos do.

Due to time constraints, the team decided it would be preferable to work with the servo rather than order a new one. Therefore, the mechanism was optimised for 120 degree servo instead of the 180 that was supposed to be used. It was calculated that there was now 86.7% of total throw, and the cam would move 35mm instead of 40mm.

The phenolic body tube was not dimensioned as expected. Websites usually specify the width as ID, which is why it was assumed that the 65mm on the website would give the internal tube dimensions as neither outer dimension (OD) nor inner dimension (ID) was specified in the product description. The width was actually the OD, and the ID was found to be 61mm. All initial CAD renders had been made with the belief that the inner diameter would be 61mm. This proved to be a minor, setback. All renders and dimensions had to be redesigned to match the body tube.

The servo mount was inserted and screwed into the body tube as a means of making it removable if need be. Nuts would be adhered on the inside and screws screwed in on the outside. However, it was found that piston could not bypass the nuts unless they were set into the plastic. As there were no holes for the nuts to be placed into, the plastic had to be melted and the nuts pushed into it.

In the future, this can be easily fixed by altering the printed design to contain gaps for the nuts.

Upon landing after a successful launch, it was discovered that one of the brake flaps had broken off the hinge mechanism. The team deduced that this was due to the flaps being open during decent due to not enough opposing force holding them closed, thus when the rocket hit the ground, the flap snapped off.

The break occurred at the epoxy seal, despite use of a 2 hour-setting variant of the adhesive. It was fixed easily for the presentation by reapplication of the adhesive, and able to be flown again

While the issue could be resolved by scoring both surfaces to be joined, the use of adhesives on the aluminium surface as a whole should be avoided in future designs, as

aluminium proves a difficult material to join with most glues and epoxies. A more permanent solution should be investigated, like securing the control surface to the hinge using mechanical fasteners like bolts or rivets. These would provide a more robust connection between the parts, but the effect of inclusion of these extra parts on the aerodynamic properties of the brakes must be investigated in detail.

Furthermore, the issue of the brakes remaining open upon landing should be addressed. Based on the acceleration data presented in this report, it can be assumed that control surfaces did not deploy during flight of the rocket, as there were no periods of anomalous deceleration evident. As such, it was likely air-flow at the high speed the vehicle was travelling at that prevented the flaps from opening.

Small magnets were not strong enough to overcome the upward force acting on the brakes during descent. Stronger magnets are an option, however, the servo may not be able to oppose the magnetic force. Electromagnets, that can be turned off when the brakes are deployed, are a suitable option. These could not be implemented into this project due to time and cost restraints.

Conclusion

The team successfully designed, implemented and flew a level 1 rocket with an onboard air braking system on an H135W motor. The air brakes functioned as intended with their opening and retraction times less than <0.5 sec. The brakes remained open for 3 seconds and their impact was directly measurable from analysing the onboard accelerometer. The brakes produced an effective 2.3x in observed drag and added ~17 N of drag. The brakes were effective in reducing altitude as a 900ft reduction in altitude was measured compared to the closed flap sim, making over a 30% reduction in altitude. This design shows potential to be scaled up to larger rockets and was proven effective throughout the project.

Recommendations

For optimal deceleration in future rockets, the design should be optimised for a 180 degree servo, rather than the 120 degree servo used in this project. The latter was used in this project due to miscommunication and lack of time to replace it. The 120 degree servo only had 86.7% of total throw. A 180 degree servo would permit for a greater deployment angle and increased drag.

While it would be ideal to create an external air braking mechanism that could be attached to any rocket as required, that simply isn't viable for this design. Therefore, a new set of air brakes would have to be implemented into every rocket. While the core design will remain the same, certain specifications such as dimensions and servo size will need to be adjusted.

The system can be modified for single flap actuation, with three servos each operating a single brake, rather than one servo operating all three. The limited diameter of this rocket meant that it was not possible to implement three servos. In larger projects this should not be a limitation.

To avoid a brake panel snapping off on future rockets, modifications have to be made to the method of adhesion. As it was, the aluminium panels were epoxied to ABS 3D printed cams. While the metal was scored before adhesion, it was not sufficient enough to provide a rigid

surface to which the epoxy could bond. Future designs should ensure strong bonding through the use of stronger epoxy resins, deeper scoring, and the use of different materials that will bond better with the epoxy.

In order to connect the deployment mechanism to the electronics sled, a long wire had to be extended the length of the rocket body. Further issue was encountered when the team realised that this cable would have to be, at a minimum, the length of the shock cord, as the nose cone would separate from the rocket body during parachute deployment.

The resulting cable was 5m long.

This posed the potential issue of delayed signals, or loss of signal. There was the risk of the cable interfering with the shock cord, or tangling with the parachute and preventing it from opening. The latter issues were mitigated through plaiting the individual cables into one, and attaching them to the shock cord using electrical tape.

To eliminate the issues relating to faulty signals, the cable length should be minimised.

Rather than extending the length of the shock cord, the cables could be designed to break at parachute deployment, as the air brakes would not longer be necessary.

Summary of the achievements of the team

The team successfully designed, constructed, and built a fully functioning air braking system.

Section 5- Manufacturing Methods

5.1: Fin manufacturing - Thomas Mackellar

During the construction of the rocket only two materials were considered for the fins, this was 3mm acrylic and 4mm plywood. The material constraints was that it had to be able to be laser cut. Laser cutting was selected as the manufacturing method as it improves accuracy over hand cutting fins, is quicker and allows for greater efficiency of material usage due to the stacking of the parts.

Plywood was chosen over acrylic due to the brittle nature of acrylic and the easy post processing ability of plywood, when epoxying and sanding. If a brittle material was selected as fin material then the fins risk breaking during landing. The overall manufacturing process is outlined using a block diagram in figure 5.1.

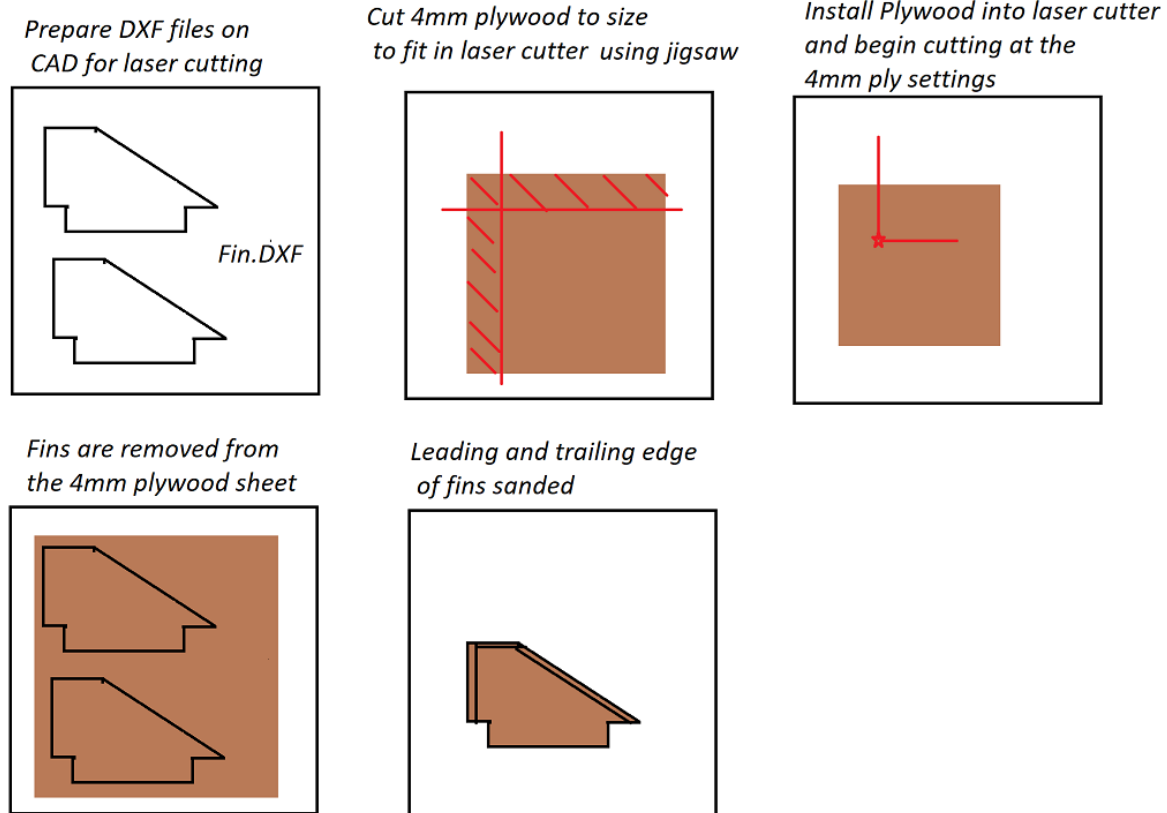


Figure 5.1: Fin manufacturing process

Once the DXF profile has been generated and the plywood cut to size, the laser cutter is set to the correct settings and precisely cuts the fins from the plywood sheet. The cut fins then have their leading and trailing edges rounded as to improve the aerodynamic properties.

5.2: Avionics Sed- Siddhant Tandon

The avionics sled was made out of 4mm thick plywood. It was laser cut (including all holes) and prepared for assembly by having its edges sanded, and holes widened, as it was observed in some cases they had been cut slightly too small to comfortably contain the M3 bolts. The process used when fabricating these components is summarised in figure 5.2:

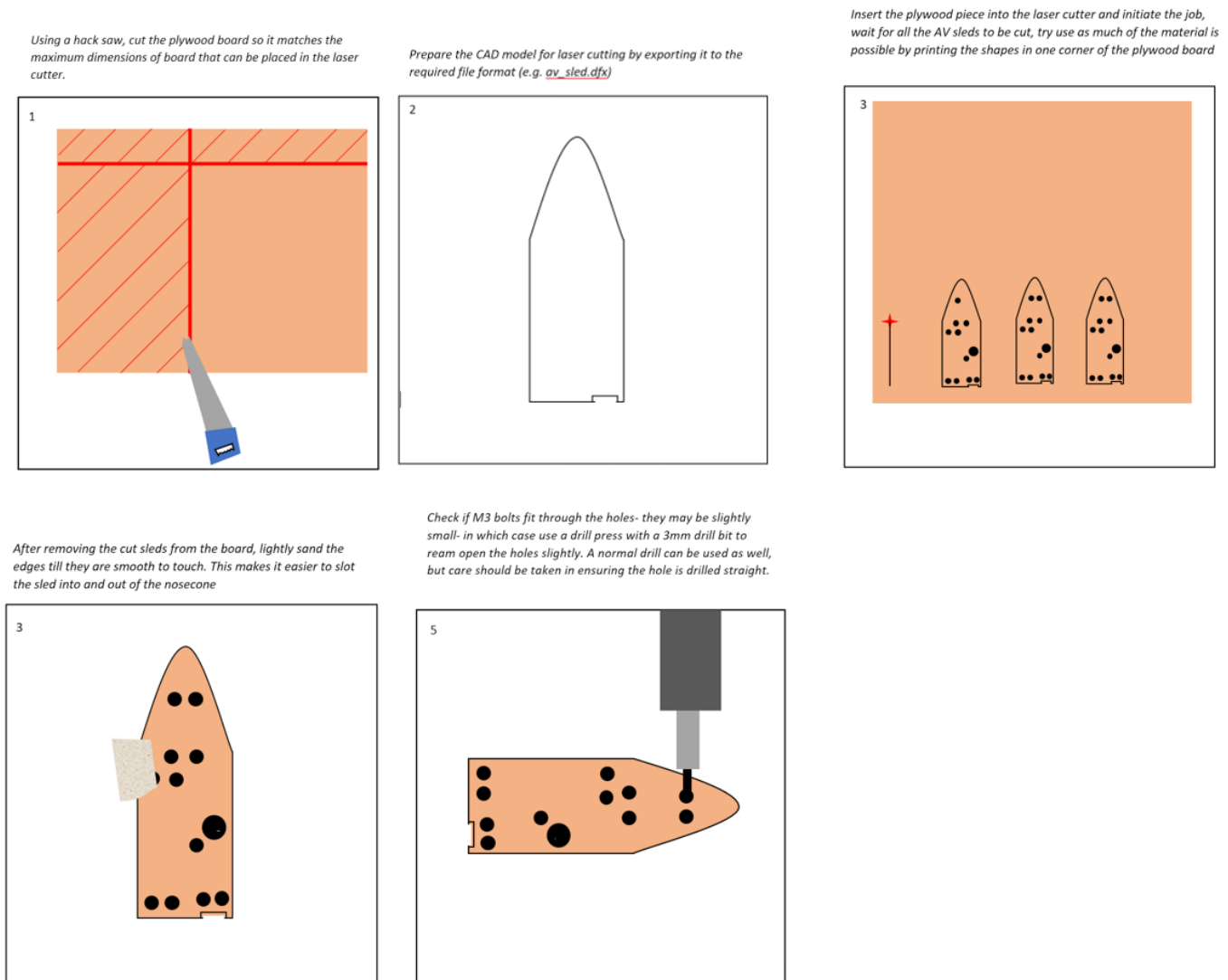


Figure 5.2: Avionics Sled manufacturing process

5.3: 3D Printed ABS Cams - Nicole Tryndoch

Before manufacturing began, it was decided that the cams would be 3D printed. This allowed for the exact shape to be designed and printed to exact specifications. Furthermore, the small size meant that this was the easiest approach.

Due to being close to the motor, and being in contact with the motor mount, melting plastic was a potential issue. This is why ABS was chosen as the material over PLA, with a higher melting point, there was less risk of the cams deforming or adhering to the motor mount during the motor burn.

The manufacturing process is outlined in figure 5.3.

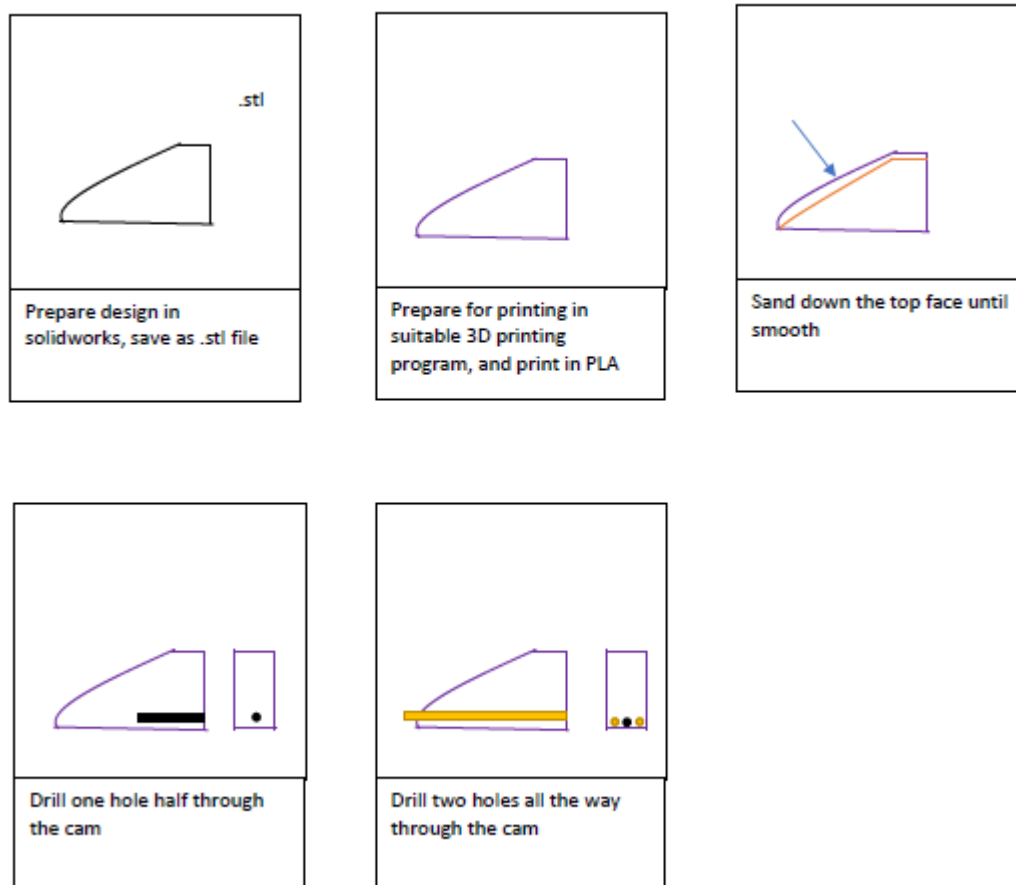


Figure 5.3: Cam manufacturing process

6.0: References

- [1]"Aerospacweb.org | Ask Us - Rocket Nose Cones and Altitude", *Aerospacweb.org*, 2019. [Online]. Available: <http://www.aerospacweb.org/question/aerodynamics/q0151.shtml>. [Accessed: 31- May- 2019].
- [2]"Selecting Between I2C and SPI for Your Project", *Lifewire*, 2019. [Online]. Available: <https://www.lifewire.com/selecting-between-i2c-and-spi-819003>. [Accessed: 31- May- 2019].
- [3] SolidWorks 2019. Paris, France: Dassault Systemes, 2019.

Appendices

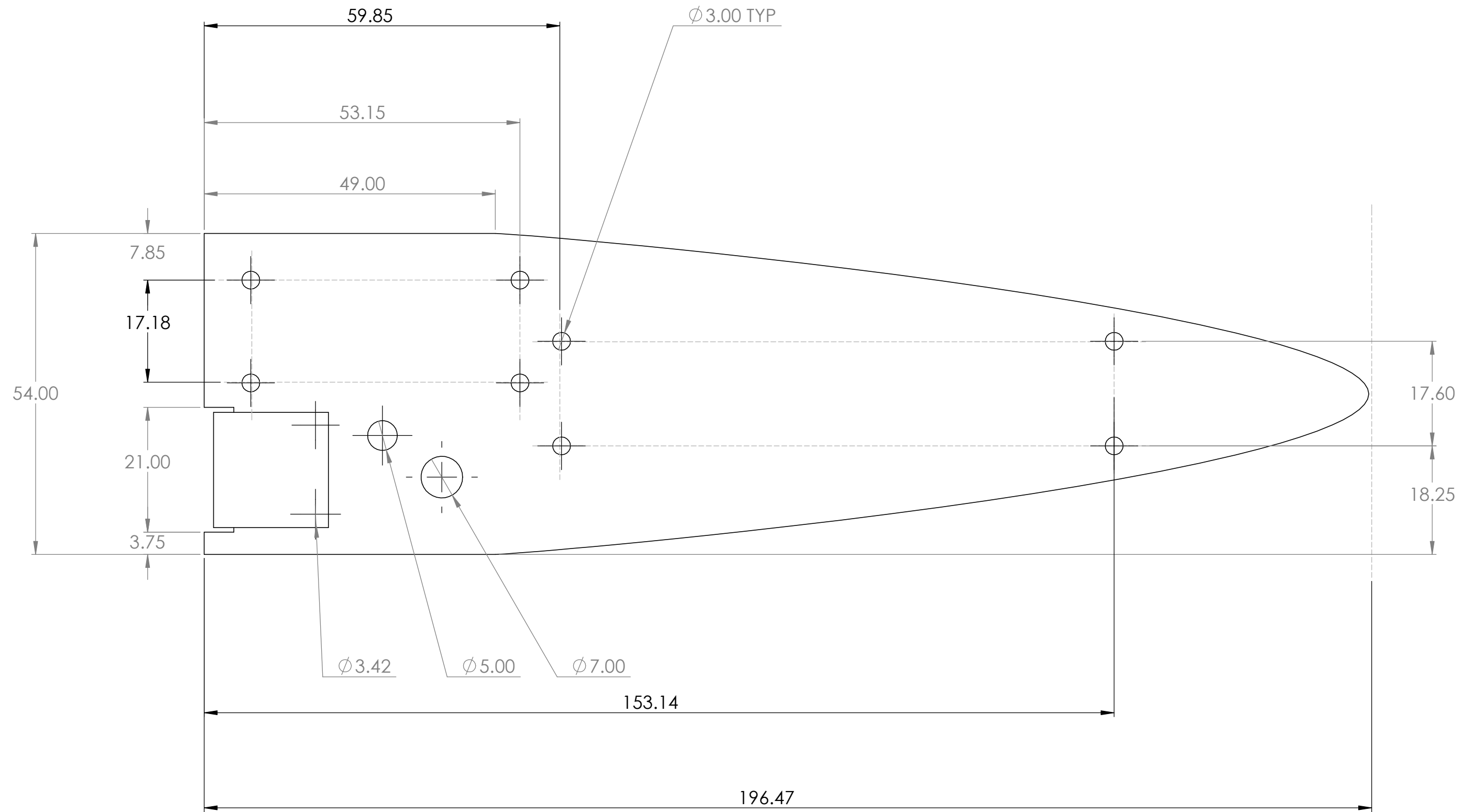
Appendix A: Budget and Cost Breakdown

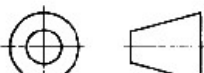

Table A.1- Breakdown of expenses during the project

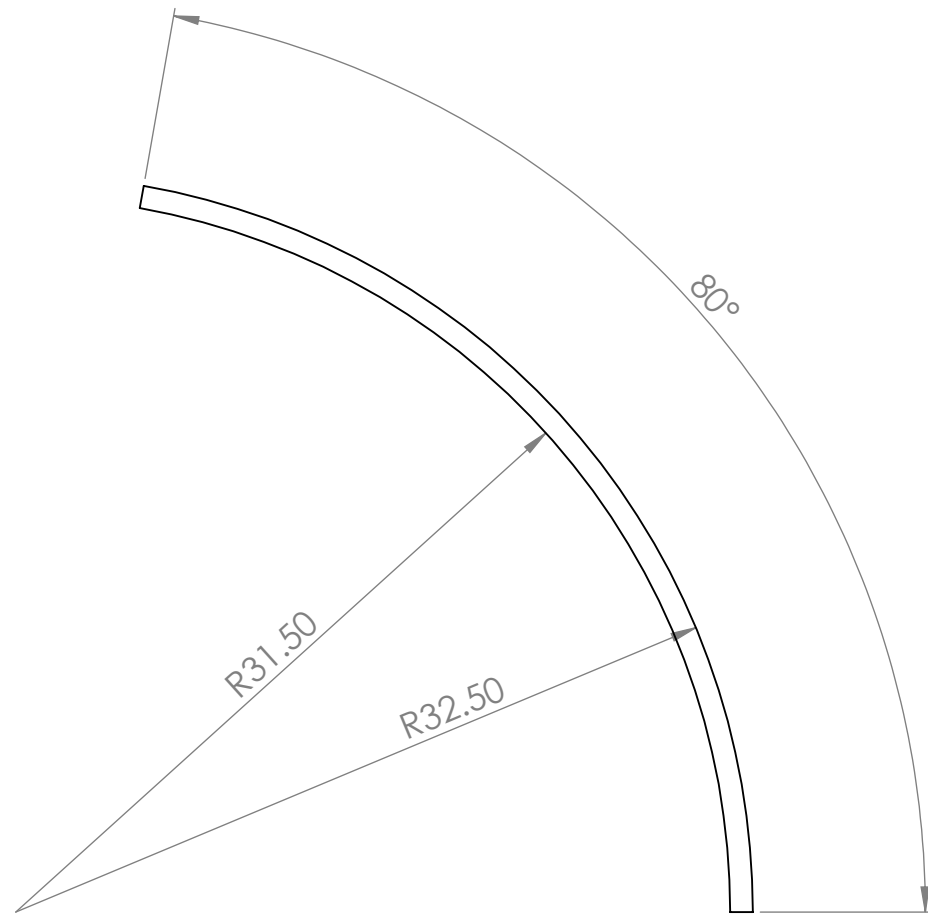
Item	Number of Items	Cost of Single Item (Dollars \$)	Overall Cost (Dollars \$)
Phenolic Tubing	1	17.00	17
Motor	1	55.00	55
Servo	1	59.00	59
Aluminium Sheet	1	4.00	4
Shock Cord	1	5.50	5.5
Eye Screw	1	1.80	1.8
Fasteners	multiple	-	5
2mm * 300mm steel rods	5	0.5	2.5
ABS filament	300g	2\$/100g	6
PLA filament	200g	2\$/100g	4
Adalogger	1	37.9	37.5
16gb sd card	1	15.8	15.8
2s 950mah lipo	1	9.5	9.5
Buck converter	1	4.5	4.5
4mm plywood	1	7.0	7.0
Switch	1	1.0	1.0
Total cost			\$235.1

Appendix B: Material Choices for various components*Table B.1- Summary of the materials used for various components of the test rocket.*

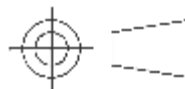
Material	Components
Phenolic tubing	Rocket body, motor mount
Aluminium sheet metal	Air brake panels
PLA	Nose cone, screw in thingy
ABS	Servo mount, centering rings, actuation mechanism
Plywood	Fins, sled
2mm steel rod	Actuator rods and guide rods for cams



NOTES: Unless otherwise specified All dimensions in mm General tolerances: Linear: ±0.2mm Angular: ±0.1° Holes were laser cut Parabolic profile of nose cone was defined by equation $y=4x^2$	MATERIAL: 3MM PLYWOOD		DRAWN: SIDDHANT TANDON		MONASH UNIVERSITY FACULTY OF ENGINEERING			
			APPROVED: THOMAS MACKELLAR		TITLE: AVIONICS SLED			
			SUBMITTED: 25/05/2019					
		DATE: 25/05/2019	DRAWING PRACTICE: AS 1100		SCALE: 3:2	SIZE: A3	DWG No: AV_1	



NOTES: AS1100
ALL UNITS mm GENERAL
TOLLERANCE $\pm 0.5\text{mm}$
 $\pm 1\text{DEGREE}$. To be made
by rolling 1mm Al1060 sheet



TITLE:

AIR BRAKE FLAP

MATERIALS:
1mm 1060AL sheet.

MONASH UNIVERSITY DEPARTMENT
OF MECHANICAL ENGINEERING

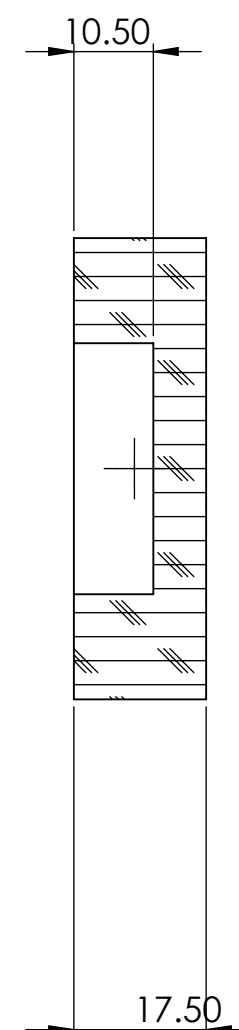
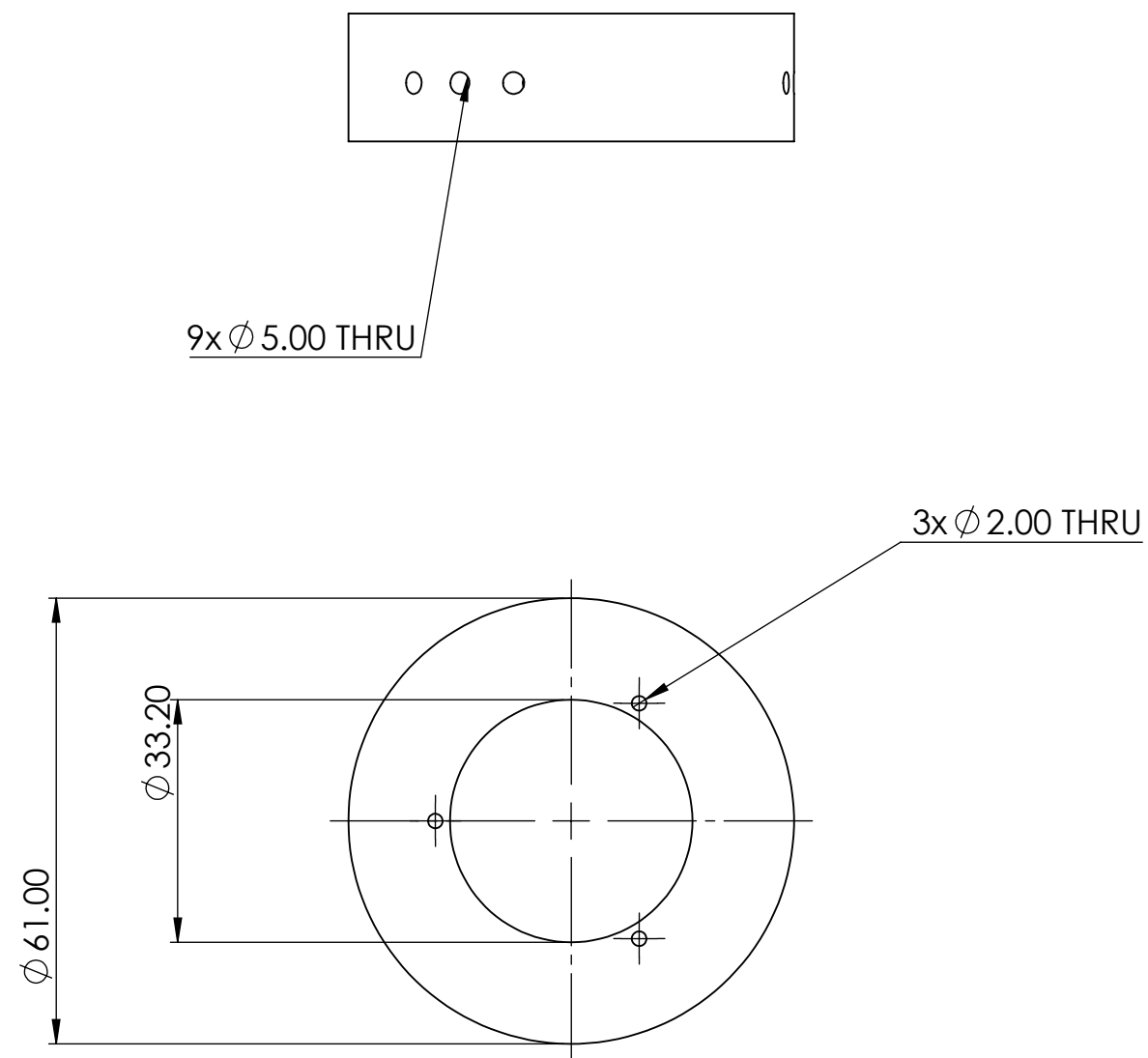
DRN BY: THOMAS MACKELLAR

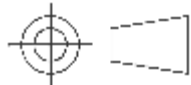
DATE:
30/5/19

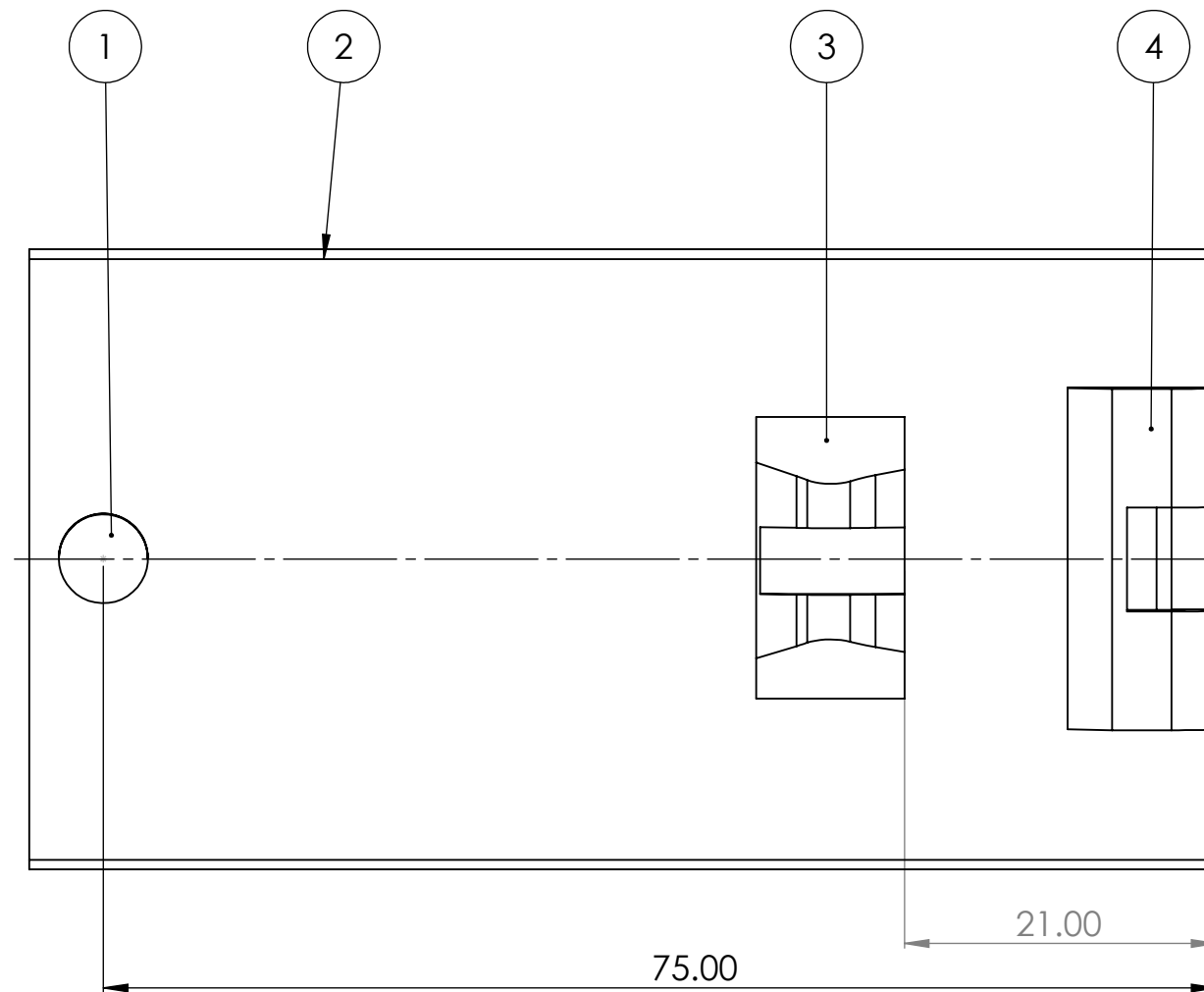
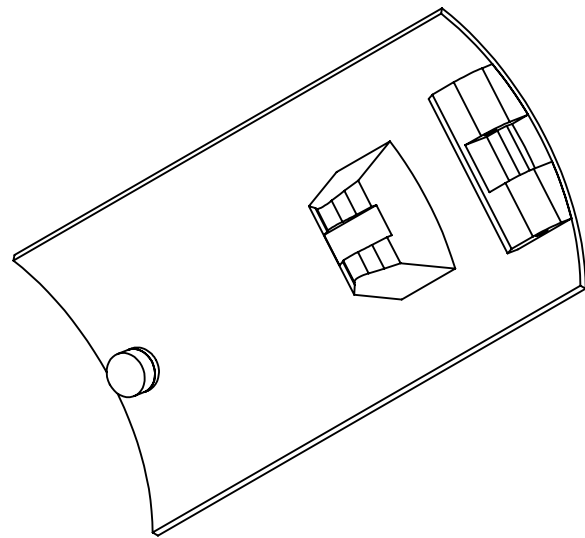
A3

SCALE: 3:1

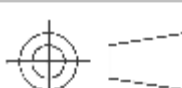
DWG NO. P01_ABF-01

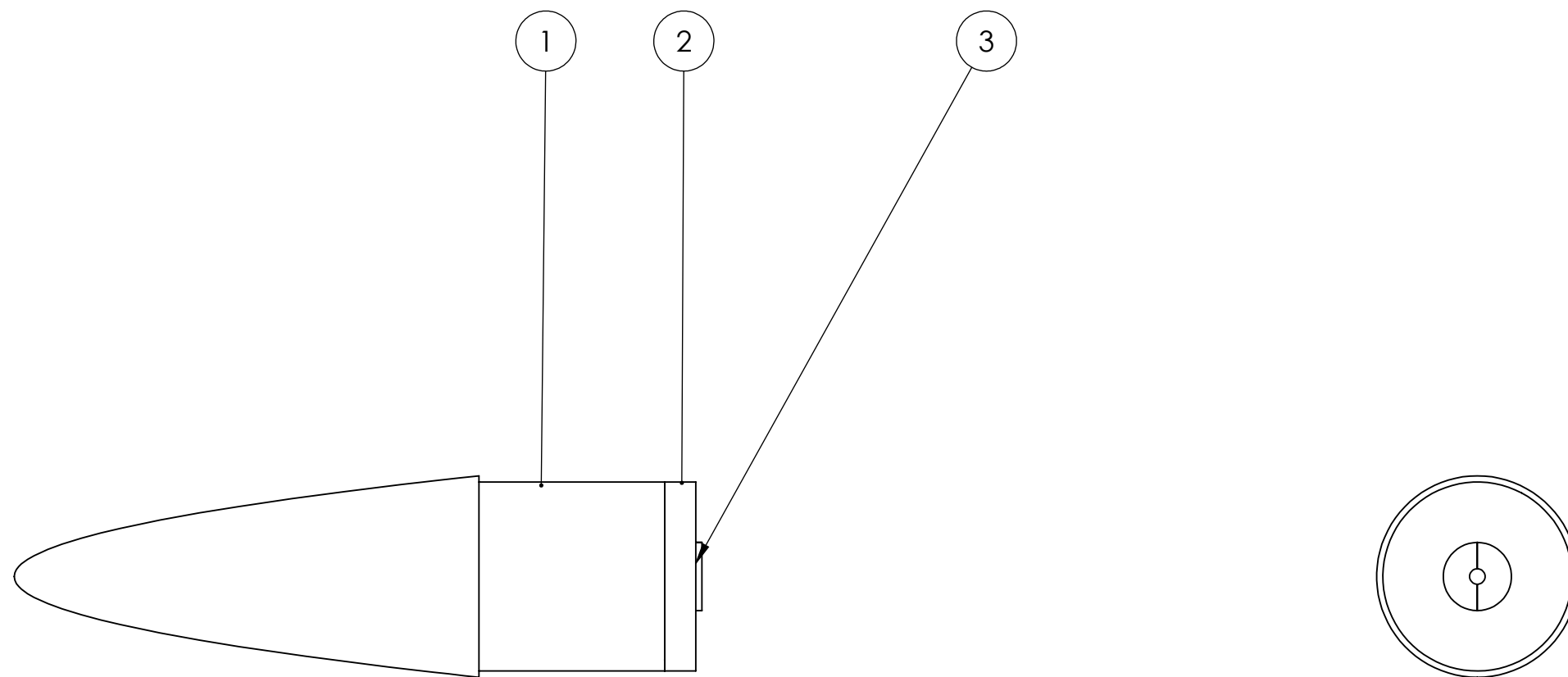


NOTES: mm Tol: 0.05mm	TITLE: BULKHEAD			
	MATERIALS: PLYWOOD	MONASH UNIVERSITY DEPARTMENT OF MECHANICAL ENGINEERING	DATE: 31/05/19	A3 SCALE: 1:1
		DRN BY: NICOLE TRYNDUCH		DWG NO. 3




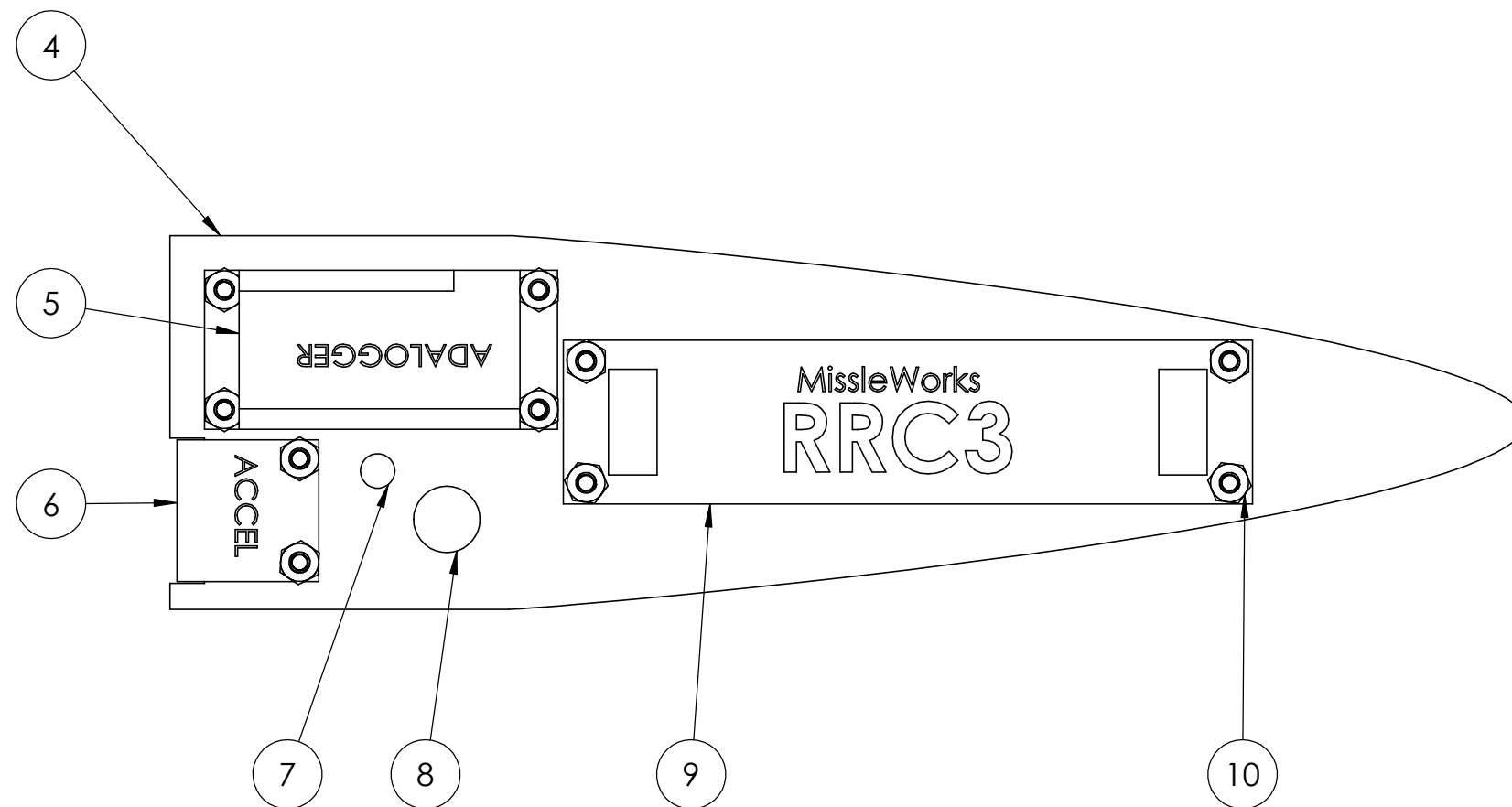
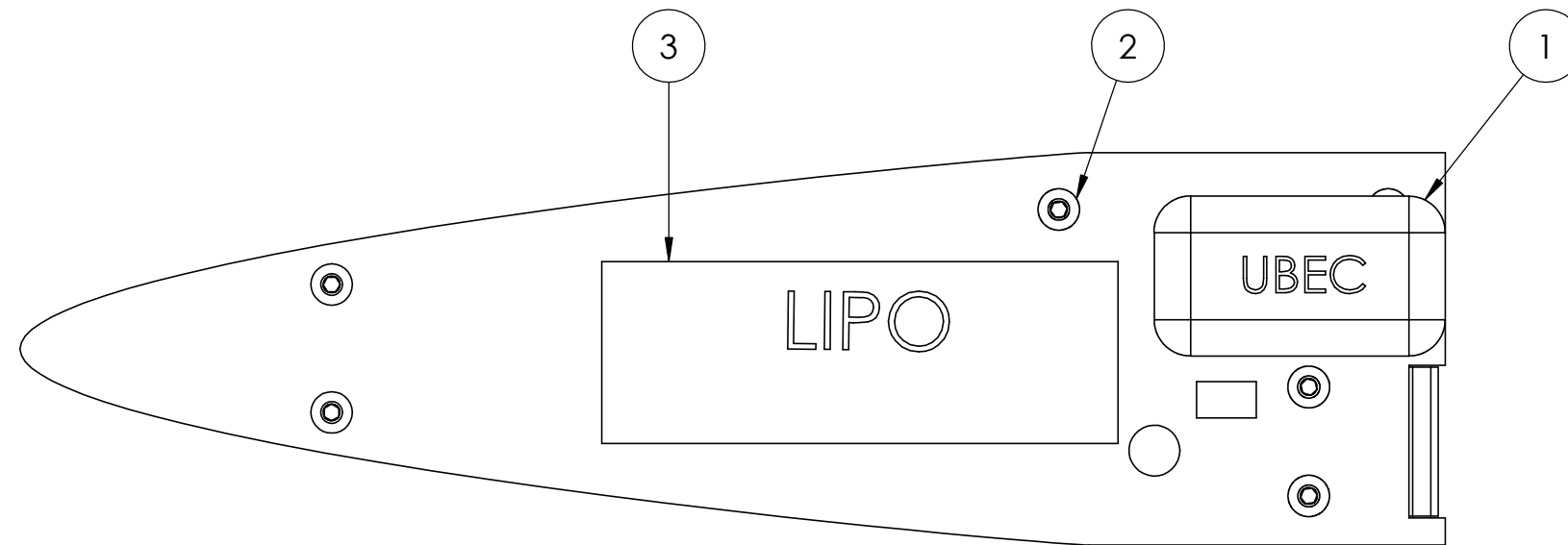
4	ABS FLAP PIVOT	1	P03_AB-F01
3	ABS CAM FOLLOWER	1	P02_AB-F01
2	ALUMINIUM AIR BRAKE FLAP	1	P01_AB-F01
1	5MM NEODYMIUM MAGNET	1	PURCH
ITEM NO.	DESCRIPTION	QTY	DRG NO

NOTES: Unless stated tolerance +/- 0.5mm. All parts to be joined using epoxy resin. AS1100 drawing standard.		TITLE: FLAP ASSEMBLY			
	MATERIALS: SEE BILL OF MATERIALS. JOINED WITH 2 PART EPOXY	MONASH UNIVERSITY DEPARTMENT OF MECHANICAL ENGINEERING		DATE: 30/5/19	A3
		DRN BY: THOMAS MACKELLAR		SCALE: 2:1	
		DWG NO. AB-F01			

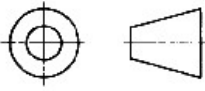



ITEM NO.	PART NUMBER	DESCRIPTION	QTY.
1	NOSE CONE	PLA	1
2	NOSE CONE CAP	PLA	1
3	BP SEAL	PLA	2

NOTES: mm Tol: 0.05mm		TITLE: NOSE CONE			
	MATERIALS: PLA	MONASH UNIVERSITY DEPARTMENT OF MECHANICAL ENGINEERING		DATE: 31/05/19	A3
		DRN BY: NICOLE TRYNDUCH		SCALE: 1:	
				DWG NO. 4	



ITEM NO.	DESCRIPTION	QTY.	MATERIAL
10	M3 Hex Nut	10	PURCH.
9	MissileWorks RRC3	1	PURCH.
8	Test Button	1	PURCH.
7	Main Power Switch	1	PURCH.
6	Adafruit LIS3DH	1	PURCH.
5	Adafruit Adalogger M0	1	PURCH.
4	Sled	1	PLYWOOD/DRAWING 001
3	LiPo	1	PURCH.
2	M3x10	10	PURCH.
1	UBEC	1	PURCH.

<p>NOTES: Unless otherwise specified All dimensions in mm General tolerances: Linear: ±0.2mm Angular: ±0.1°</p>	<p>MATERIAL: View Bill of Materials</p>		DRAWN: SIDDHANT TANDON		MONASH UNIVERSITY FACULTY OF ENGINEERING			
			APPROVED: THOMAS MACKELLAR		TITLE: AVIONICS SLED ASSEMBLY			
			SUBMITTED: 25/05/2019					
		DATE: 25/05/2019	DRAWING PRACTICE: AS 1100	SCALE: 1:1	SIZE: A3	DWG No: 4		SHT: 1